

NASA TECHNICAL
MEMORANDUM

NASA TM X-64671

CASE FILE
COPY

PROBABILITY OF SATELLITE COLLISION

By James W. McCarter
Aero-Astroynamics Laboratory

June 8, 1972

NASA

*George C. Marshall Space Flight Center
Marshall Space Flight Center, Alabama*

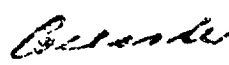
1. REPORT NO. TM X-64671		2. GOVERNMENT ACCESSION NO.		3. RECIPIENT'S CATALOG NO.	
4. TITLE AND SUBTITLE Probability of Satellite Collision				5. REPORT DATE June 8, 1972	
				6. PERFORMING ORGANIZATION CODE	
7. AUTHOR(S) James W. McCarter				8. PERFORMING ORGANIZATION REPORT #	
9. PERFORMING ORGANIZATION NAME AND ADDRESS George C. Marshall Space Flight Center Marshall Space Flight Center, Alabama 35812				10. WORK UNIT NO.	
				11. CONTRACT OR GRANT NO.	
				13. TYPE OF REPORT & PERIOD COVERED Technical Memorandum	
12. SPONSORING AGENCY NAME AND ADDRESS National Aeronautics and Space Administration Washington, D. C. 20546				14. SPONSORING AGENCY CODE	
15. SUPPLEMENTARY NOTES Prepared by Aero-Astroynamics Laboratory, Science and Engineering					
16. ABSTRACT A method is presented for computing the probability of a collision between a particular artificial earth satellite and any one of the total population of earth satellites. The collision hazard incurred by the proposed modular Space Station is assessed using the technique presented. The results of a parametric study to determine what type of satellite orbits produce the greatest contribution to the total collision probability are presented. Collision probability for the Space Station is given as a function of Space Station altitude and inclination. Collision probability was also parameterized over miss distance and mission duration.					
17. KEY WORDS Collision Space Station Satellite Collision Orbital Debris Interference Satellite Collision Probability Space Station Collision Hazard Space Station Collision Probability Collision Probability Computation Techniques				18. DISTRIBUTION STATEMENT UNCLASSIFIED-UNLIMITED  E. D. Geissler Director, Aero-Astroynamics Lab, MSFC	
19. SECURITY CLASSIF. (of this report) Unclassified		20. SECURITY CLASSIF. (of this page) Unclassified		21. NO. OF PAGES 65	
				22. PRICE \$3.00	

TABLE OF CONTENTS

	Page
SUMMARY	1
INTRODUCTION	2
PROBLEM DESCRIPTION	2
MATHEMATICAL FORMULATION	4
SAMPLE PROBLEM	16
RESULTS	16
CONCLUSIONS	24
APPENDIX A: DERIVATION OF RELATIVE VELOCITY COMPONENTS \dot{X} , \dot{Y} , \dot{Z} AND ORIENTATION ANGLES OF DEBRIS PATH θ AND β	31
APPENDIX B: DERIVATION OF COLLISION DISTANCE, d	38
APPENDIX C: AREA DETERMINATION OF PROBABILITY VERSUS ω HUMP	41
APPENDIX D: MATHEMATICAL JUSTIFICATION FOR ELLIPTICAL APPROXIMATION OF INTEGRAL	44
APPENDIX E: EXTENSION OF PROBABILITY PER LAP EXPRESSION TO PROBABILITY FOR THE ENTIRE MISSION	50
APPENDIX F: COLLISION PROBABILITY BETWEEN THE TARGET SATELLITE AND ANY ONE OF THE TOTAL NUMBER OF DEBRIS SATELLITES	51
APPENDIX G: DETERMINATION OF THE ANGLE BETWEEN TWO ORBIT PLANES	52
REFERENCE	55

LIST OF ILLUSTRATIONS

Figure	Title	Page
1.	Orbital geometry for a collision situation between two orbiting objects	3
2.	Relative coordinate system	4
3.	Net position change of the target satellite during one orbital period of the debris satellite	6
4.	Successive passes of the debris satellite through the target satellite orbit plane as viewed in the relative coordinate system	7
5.	Positions of the orbit plane intersection line which produce collision possibilities	9
6.	Geometrical description of the collision distance, d	10
7.	Geometrical explanation of collision probability expression.	11
8.	Illustration of typical trend in probability vs ω (or η) curve	13
9.	Trends in P_{lap} vs ω curve when apogee and/or perigee altitude of debris satellite is near target altitude.	14
10.	Total collision probability as a function of Space Station altitude.	17
11.	Total collision probability as a function of Space Station altitude, h_{ss} , and the number of debris objects which cross h_{ss}	19
12.	Total collision probability as a function of Space Station orbit inclination.	20
13.	Probability of collision with individual debris objects as a function of perigee altitude of the debris orbit.	21

LIST OF ILLUSTRATIONS (Concluded)

Figure	Title	Page
14.	Probability of collision with individual debris objects as a function of apogee altitude of the debris orbit	22
15.	Variation of collision probability for an individual debris object as perigee altitude is varied through the target altitude.	23
16.	Effect of out-of-plane angle, δ , on collision probability for some typical debris orbits holding apogee altitude constant	25
17.	Effect of out-of-plane angle, δ , on collision probability for some typical debris orbits holding perigee altitude constant	26
18.	Total collision probability for Space Station as a function of miss distance (target sphere radius)	27
19.	Total collision probability for Space Station as a function of mission duration.	28
A-1.	Inertial velocity of the debris satellite	33
A-2.	Relative velocity vector, \overline{V}_r	37
D-1.	Geometrical description of the collision distance, d	45
D-2.	Edgewise view of the small circle in the target sphere defined by passage of the debris object through the target sphere.	46
G-1.	Geometrical description of the mutual orbit orientation between the debris and target orbits	53

LIST OF SYMBOLS

Symbol	Definition
A	Area under one hump of the probability versus ω curve.
C_1	The angular momentum associated with the orbit of the debris satellite.
d	A distance measured in the direction of the relative x-axis through which the path of a debris satellite can pass and intersect the target sphere.
e	Eccentricity of the orbit of the debris satellite.
h_{ss}	Altitude of the proposed modular Space Station.
\bar{i}	Unit vector in the relative x direction.
i_d	Inclination of the orbit of the debris satellite.
i_t	Inclination of the orbit of the target satellite.
i'_t	Supplement of i_t .
j	Counting index for debris satellites.
k	Total number of debris satellites in earth orbit.
L	Total number of laps that occur between the target satellite and a debris satellite during an entire mission.
P_{lap}	Probability of collision between the target satellite and the debris satellite - each lap for a constant mutual orbit plane orientation.
\bar{P}_{lap}	Probability of collision between the target satellite and the debris satellite - each lap averaged over all possible arguments of perigee and node separations.

LIST OF SYMBOLS (Continued)

Symbol	Definition
P_m	Probability of collision between the target satellite and the debris satellite for the entire mission.
$P_{\max.}$	Maximum collision probability obtained as argument of perigee is varied from 0 deg to 360 deg.
P_{nc}	Probability of noncollision.
P_{TOT}	Probability that the target satellite will collide with any debris satellite at least once during the mission.
p	Semilatus rectum of the orbit of the debris satellite.
R	Radius of the target sphere.
R_A, R_p	Radii of apogee and perigee of the debris satellite orbit.
\bar{R}_d	Inertial position vector of the debris satellite.
$R_{d_1, 2}$	Magnitudes of debris satellite position vector at the line of intersection when the probability versus ω curve goes to zero.
\bar{R}_t	Inertial position vector of the target satellite.
r	Radius of the small circle which is defined by the intersection of the plane of debris satellite passes with the target sphere in the relative coordinate system.
T_t	Orbital period of the target vehicle.
u	Argument of latitude of the line of intersection between the orbit planes measured in the plane of the debris orbit.
∇_d	Inertial velocity of the debris satellite.

LIST OF SYMBOLS (Continued)

Symbol	Definition
$\Delta\eta$	The interval of η for which a nonzero collision probability exists.
$\Delta\Psi$	Angular range about the line of intersection between the debris and target orbit planes in which the target satellite can contact the debris object.
$\Delta\Omega$	The difference in the ascending nodes of the debris and target satellites.
$\Delta\omega$	The interval of ω for which a nonzero collision probability exists.
δ	Angle between the orbit planes of the debris and target satellites.
ϵ	Angle between the path of the debris satellite and the relative x-axis as the debris satellite passes through the orbit plane of the target satellite.
η	The "True Anomaly" of the line of intersection between the debris and target orbit planes measured in the debris orbit plane.
$\eta_{\max.}$	The value of η at which the collision probability is a maximum (for constant $\Delta\Omega$).
θ	Angle between the projection of \bar{V}_r onto the relative x-z plane and the x axis.
λ	Angle between the ascending node line of the debris satellite and the line of intersection between the debris and target orbit planes.
μ	Gravitational constant of the earth, $3.986032 \times 10^{14} \text{ m}^3/\text{sec.}$

LIST OF SYMBOLS (Continued)

Symbol	Definition
\bar{V}_r	Relative velocity between the debris satellite and the target satellite.
\bar{V}_t	Inertial velocity of the target satellite.
x, y, z	Coordinates of a point of intersection between the target sphere and the line of travel of the debris satellite in the relative coordinate system.
x_d, y_d	Coordinates of the point where the debris satellite passes through the target orbit plane.
$\dot{x}, \dot{y}, \dot{z}$	Relative velocity components of the debris satellite in the relative coordinate system.
$\dot{x}_d, \dot{y}_d, \dot{z}_d$	Inertial velocity components of the debris satellite.
x_{d1}, x_{d2}	x coordinates in the relative coordinate system of the point where the debris trajectory passes through the target orbit plane and is tangent to the target sphere.
$\dot{x}_t, \dot{y}_t, \dot{z}_t$	Inertial velocity components of the target satellite.
α	Orientation angle of the small circle in the target sphere defined by successive passes of the debris satellite through the target orbit plane.
β	Angle between the projection of \bar{V}_r onto the relative x-y plane and the x axis.
γ	Flight path angle of the debris satellite as passage through the target orbit plane occurs.
ΔS	Net change in the position of the target satellite relative to the position of the debris satellite during one orbital period of the debris satellite (measured as a path length) .

LIST OF SYMBOLS (Concluded)

Symbol	Definition
$\bar{\rho}$	The relative position vector of the debris satellite in the relative coordinate system.
ρ_x, ρ_y, ρ_z	The x, y, and z components of $\bar{\rho}$.
σ	Angle between the ascending node line of the target satellite and the line of intersection between the debris and target orbit planes.
ω	Argument of perigee of the debris orbit measured from the ascending node to the radius of perigee.
$\omega_{\max.}$	The argument of perigee at which the collision probability is a maximum (for constant $\Delta\Omega$).
$\bar{\omega}_t$	Angular velocity of the target satellite.
$\omega_x, \omega_y, \omega_z$	The rotational rates of the relative coordinate system about the x, y, and z axes, respectively.

PROBABILITY OF SATELLITE COLLISION

SUMMARY

A technique for computing the probability that a collision will occur between a given satellite (target satellite) and any one of the total population of debris satellites is presented. This method is restricted to near-circular target satellite orbits. The following assumptions were made:

1. The satellite sample consists only of objects trackable by North American Air Defense Command (NORAD).
2. The satellite population remains static as of a certain epoch.
3. Effects of aerodynamic drag, solar wind, and deliberate propulsive maneuvers are neglected.
4. The target satellite and debris satellite ascending nodes are random over 360 deg.
5. The arguments of perigee of the debris satellites are random over 360 deg.
6. The position of lapping between the target satellite and each debris satellite is random over 360 deg.
7. The radius of apogee, radius of perigee, and inclination of each debris satellite and the target satellite remain constant.

In order to make the probability calculations, each debris satellite was analyzed separately, and the total probability of collision was determined from the individual probabilities of each debris satellite.

A realistic sample problem (the proposed modular Space Station) is presented to provide further insight into the collision problem. A satellite sample of September 1970 containing 1805 objects was used. For a Space Station mission of 10 yr and an inclination of 55 deg, the collision probability varied from approximately 0.01 to 0.04 over the altitude range being considered for the Space Station.

The results of a parameter study to determine what types of debris orbits (size and shape) contribute a large part to the total collision probability are given. Near-circular orbits which cross the target vehicle altitude contribute the most to the total collision probability.

INTRODUCTION

Man's understanding of his environment has advanced significantly with the advent of artificial earth satellites as remote sensing devices. When these instruments are launched into earth orbit, there is usually some debris (payload shrouds, explosive bolt fragments, spent stages, etc.) which accompanies them. The rate at which these objects (payloads and debris) have been placed into earth orbit has exceeded the rate at which they have fallen back to earth (due to orbital decay), affecting a continual growth in the total number of artificial earth satellites. NORAD has identified 2588 objects in earth orbit as of October 31, 1971 [1]. If the present trend continues, this number will continue to grow.

In view of this large and increasing satellite density in earth orbital space, the question arises as to the probability of a collision between two of the satellites. This question has particular significance for manned missions since crew safety is always a high priority item. The protection of expensive, unmanned satellites (communications, meteorological, etc.) against collision with other objects would also be desirable. Decisions with regard to "safe" altitudes or necessity of collision avoidance systems might be intimately dependent on a realistic assessment of the collision hazard.

This report presents a method of determining the probability that a given satellite (target satellite) will collide with any other satellite (debris satellite) in earth orbit. The computational technique is described in general terms in the text, and a realistic sample problem (the proposed modular Space Station) is analyzed to provide further insight into the collision problem. The equations are derived in the seven appendices.

PROBLEM DESCRIPTION

The method of computing collision probability for a single debris satellite with a target satellite is first shown, and is then extended to include the entire debris satellite population.

Figure 1 shows an impending collision between the target satellite and a debris satellite. Clearly, a collision possibility exists only in the vicinity where the paths of the two bodies intersect (within $\Delta\Psi/2$ as shown). This implies that both bodies must be close to the line of intersection between the

orbit planes and that their altitudes be nearly the same. Further, both bodies must be there at nearly the same time. A collision is possible only at such times that one body is in the process of lapping the other body (lapping is the acquisition of a zero phase angle between the objects).

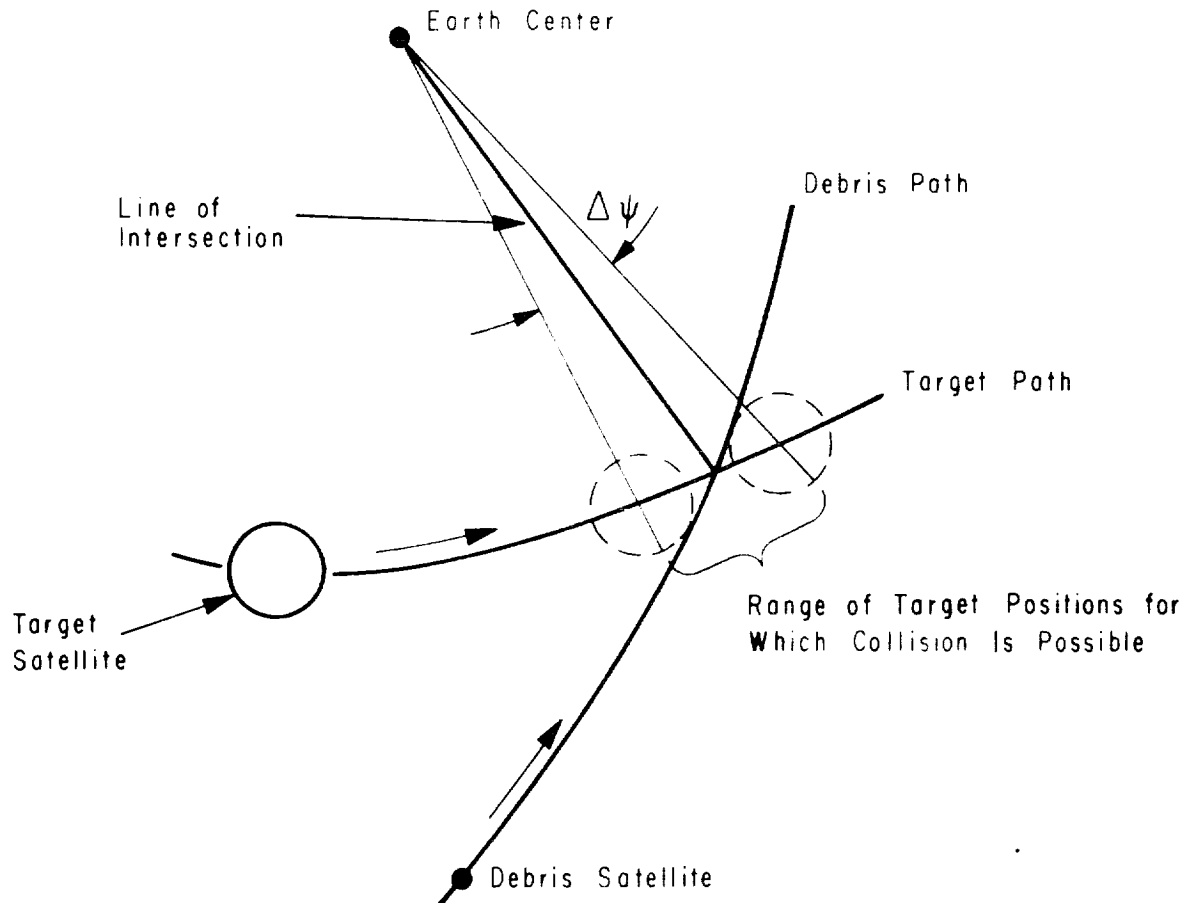


Figure 1. Orbital geometry for a collision situation between two orbiting objects.

In this study, the target satellite is simulated as a sphere of radius R . The dimensions of the debris satellite are neglected explicitly, but can be accounted for in an actual case by increasing the radius of the target sphere by an appropriate amount. If the debris satellite touches or intrudes into the sphere representing the target satellite, then a collision is defined. The immediate problem, then, is to determine the probability that this will occur.

MATHEMATICAL FORMULATION

For this problem, it is convenient to define a coordinate system at the center of the target satellite as shown in Figure 2. This coordinate system will be referred to as the "relative" coordinate system. The y axis of this system remains in the direction of the position vector \bar{R}_t , and the z axis is in the direction of the momentum vector $\bar{R}_t \times \bar{V}_t$. The x axis is a curvilinear axis which is tangent to the orbit path and remains parallel to the local horizontal. Defining the relative coordinate system in this way restricts this study to circular orbits for the target vehicle.

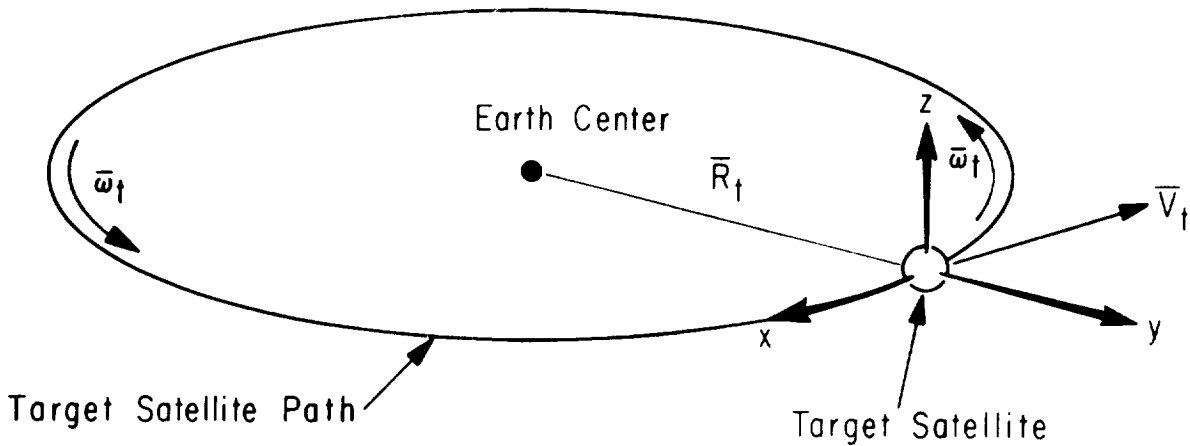


Figure 2. Relative coordinate system.

For specified orbits and a given mutual orbit plane orientation (specific values of inclinations, arguments of perigee, and ascending node separation), the velocity of the debris satellite as it passes through the orbit plane of the sphere can be determined in the relative coordinate system (Appendix A). If the path of the debris satellite is approximated as a straight line in the vicinity where collision is possible, then the direction of this relative velocity

vector represents the direction of the trajectory of the debris object. When this trajectory passes through the target sphere, a collision occurs.

The debris satellite has an opportunity to pass through the sphere only when lapping between the two objects is occurring. This is made clearer by examining Fig. 3 which shows an inertial view of the paths of the debris and target satellites. Assume that the target satellite is in position 1 when the debris satellite passes through the target orbit plane. If the period of the target satellite is less than the period of the debris satellite, then the target satellite will have traversed a complete orbit plus some distance ΔS (position 2) at the time the debris satellite passes through the target plane again. Therefore, with each successive orbit of the debris satellite, the target satellite approaches ΔS closer to the position in its orbit at which a collision can occur. This same idea is illustrated in Fig. 4 with respect to the relative coordinate system. This figure shows the debris satellite passing through the target orbit plane at an altitude difference of y_d . With each orbital period, the debris satellite passes through the target plane ΔS closer to the sphere.

In this relative reference frame (Fig. 4) there are certain characteristics common to each debris satellite pass through the target orbit plane:

1. The value of y_d (the altitude difference between the two bodies) is approximately the same each pass. The reason for this is that the altitude of the debris object during passage is determined by the position of the intersection line in the debris orbit, which in turn is determined by the argument of perigee (the angle between the ascending node and the line of perigee). Perturbations in argument of perigee due to the effects of the earth's oblateness are too slight to cause significant changes in y_d from one pass to another.
2. The direction in which the debris satellite is traveling as it passes through the target plane remains approximately the same from passage to passage. The same reason given for item 1 above also applies here since, for a given angle between the orbit planes, the direction of travel is a function of the satellite's flight path angle and the flight path angle during passage is a function of argument of perigee.
3. The distance between successive passes, ΔS , is a constant because, as stated earlier, this study is restricted to circular orbits of the target satellite. The path speed of the target satellite in circular orbits is a constant; thus, the net change in its position during one orbital period of the debris object will remain constant.

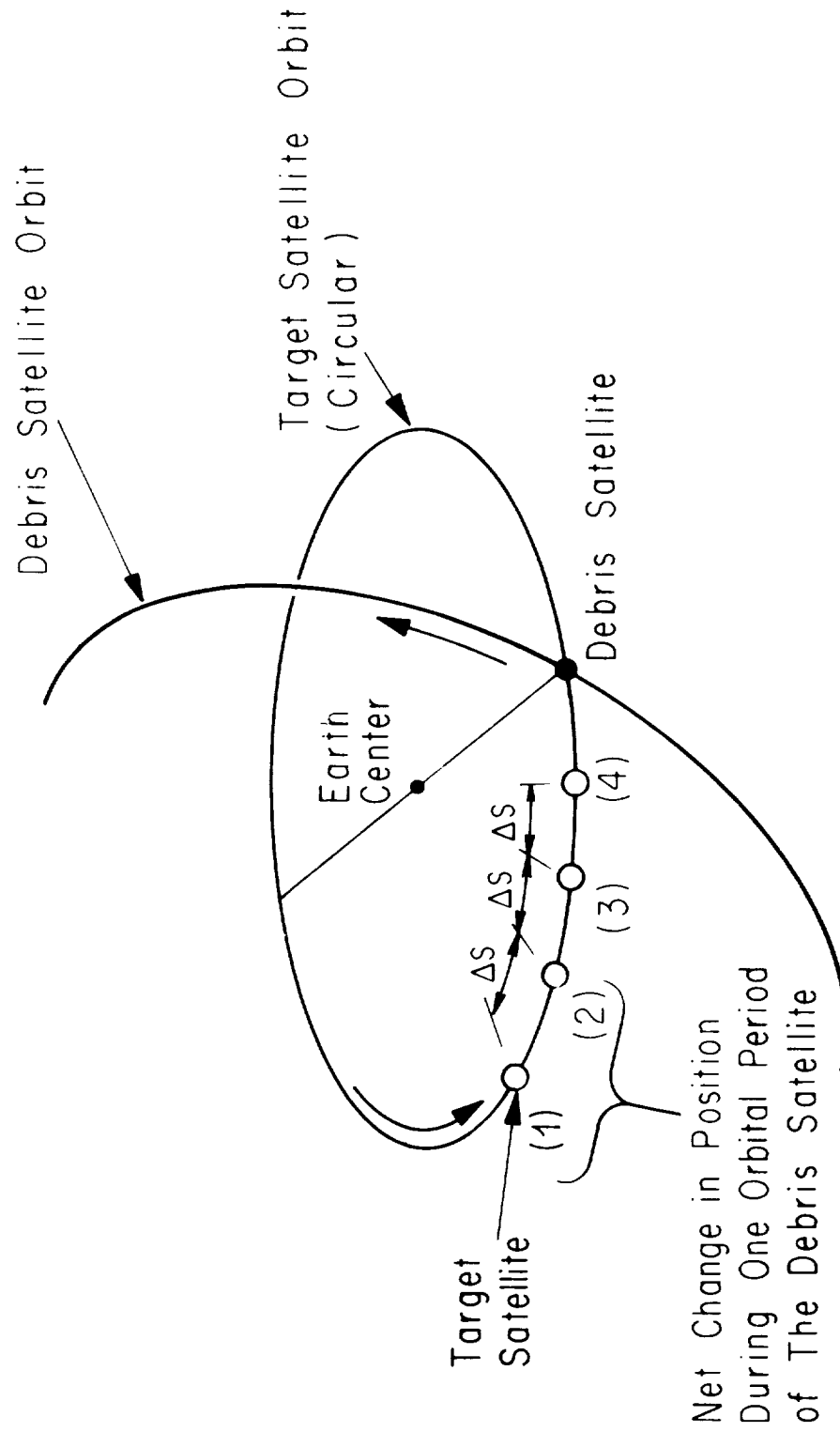


Figure 3. Net position change of the target satellite during one orbital period of the debris satellite.

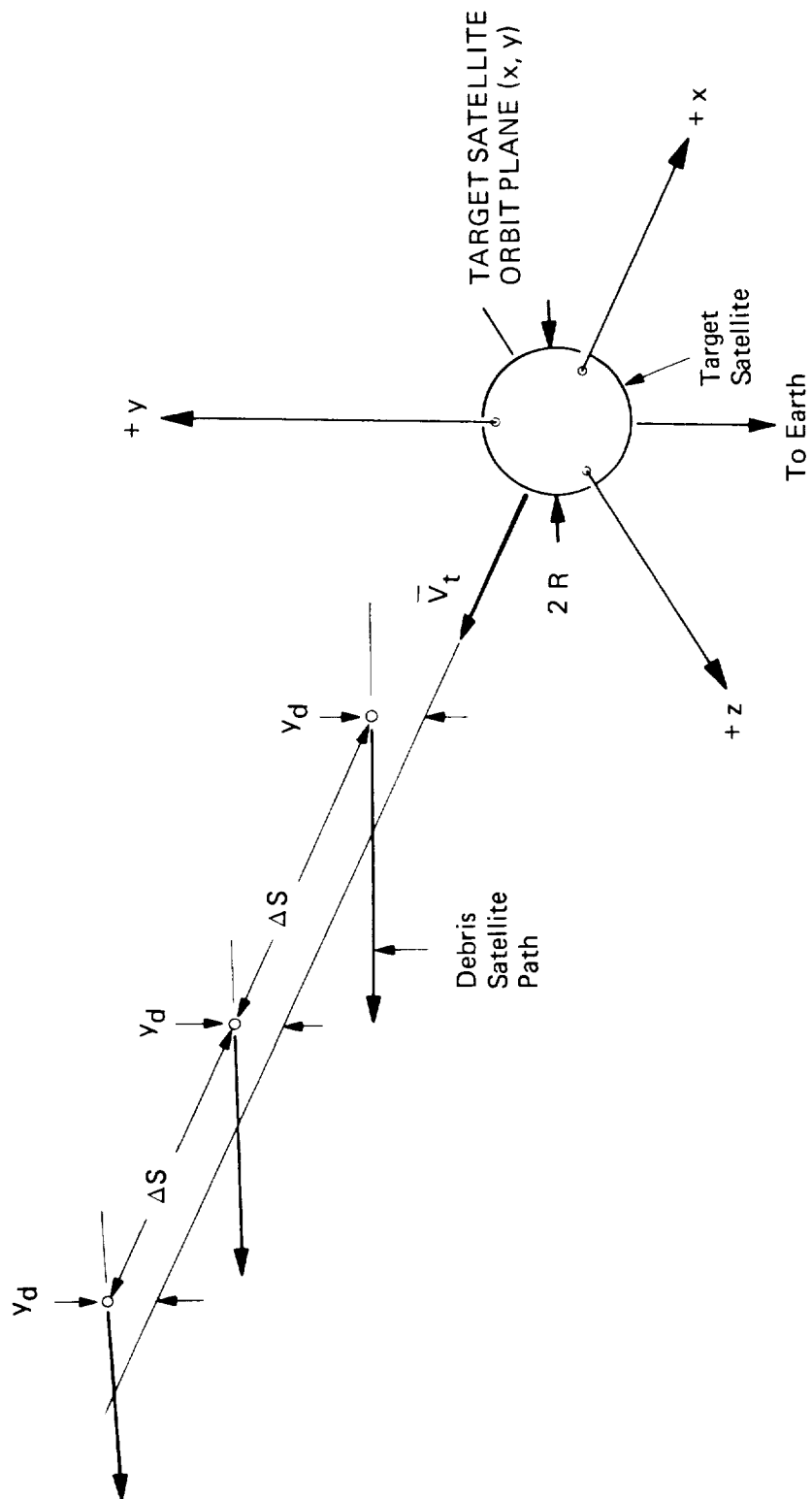


Figure 4. Successive passes of debris satellite through target satellite orbit plane as viewed in the relative coordinate system.

4. The path of the debris satellite is almost a straight line in the vicinity of the target plane where collision is possible (at least a distance $2R$ from the target plane).

Assuming that the debris satellite's R_A and R_p remain constant, the value of y_d depends upon the orientation of the major axis of the debris satellite's elliptical orbit with respect to the line of intersection; i.e., y_d depends upon the "true anomaly" of the line of intersection as measured in the debris satellite orbit plane (Fig. 5). Most orientations, as represented by the dashed line in Figure 5, will cause y_d to be of such a value that it would be impossible for the trajectory of the debris satellite to pass through the target sphere. However, when the intersection line occurs within some interval of true anomaly, $\Delta\eta$, approximately the position of equal altitudes (the shaded area), a non-zero collision probability exists and can be calculated in the following manner. As shown in Figure 6, there will be a certain interval (d) along a line parallel to the relative x axis, such that if the trajectory of the debris object intersects the target orbit plane within this interval, the trajectory will pass through the target sphere. The exact value of d is dependent upon the value of y_d and the three-dimensional direction that the debris satellite is traveling. The derivation of d is given in Appendix B.

Once this collision distance (d) has been calculated, the probability of collision can be calculated in the following manner. In Figure 6, the successive debris passes through the target orbit plane are shown occurring at particular positions along the relative x axis. The exact positioning of these passes is actually unknown and is therefore considered to be completely random. That is, the debris satellite passes can be shifted any amount up to a distance of ΔS (after which any subsequent shift produces positions which are a repeat of a previous position), and each of these positions is equally probable to occur.

To gain insight into how the probability of collision can be calculated from this, consider the following example. Assume that the interval ΔS is divided into six equal segments of length Δx (Fig. 7) and that there are a large number of cases (say 1000) of a debris satellite passing through the target plane in any random position within ΔS . This quality of randomness dictates that the same number of passages are possible in each Δx interval, because passage through any segment of ΔS is equally probable with passage through any other segment of equal length. In Figure 7, $\Delta x = \Delta S/6$. Let m be the number of cases which can occur in the interval Δx out of the total number of cases, n , which occur within ΔS . Then

$$m = \frac{n}{6} \quad . \quad (1)$$

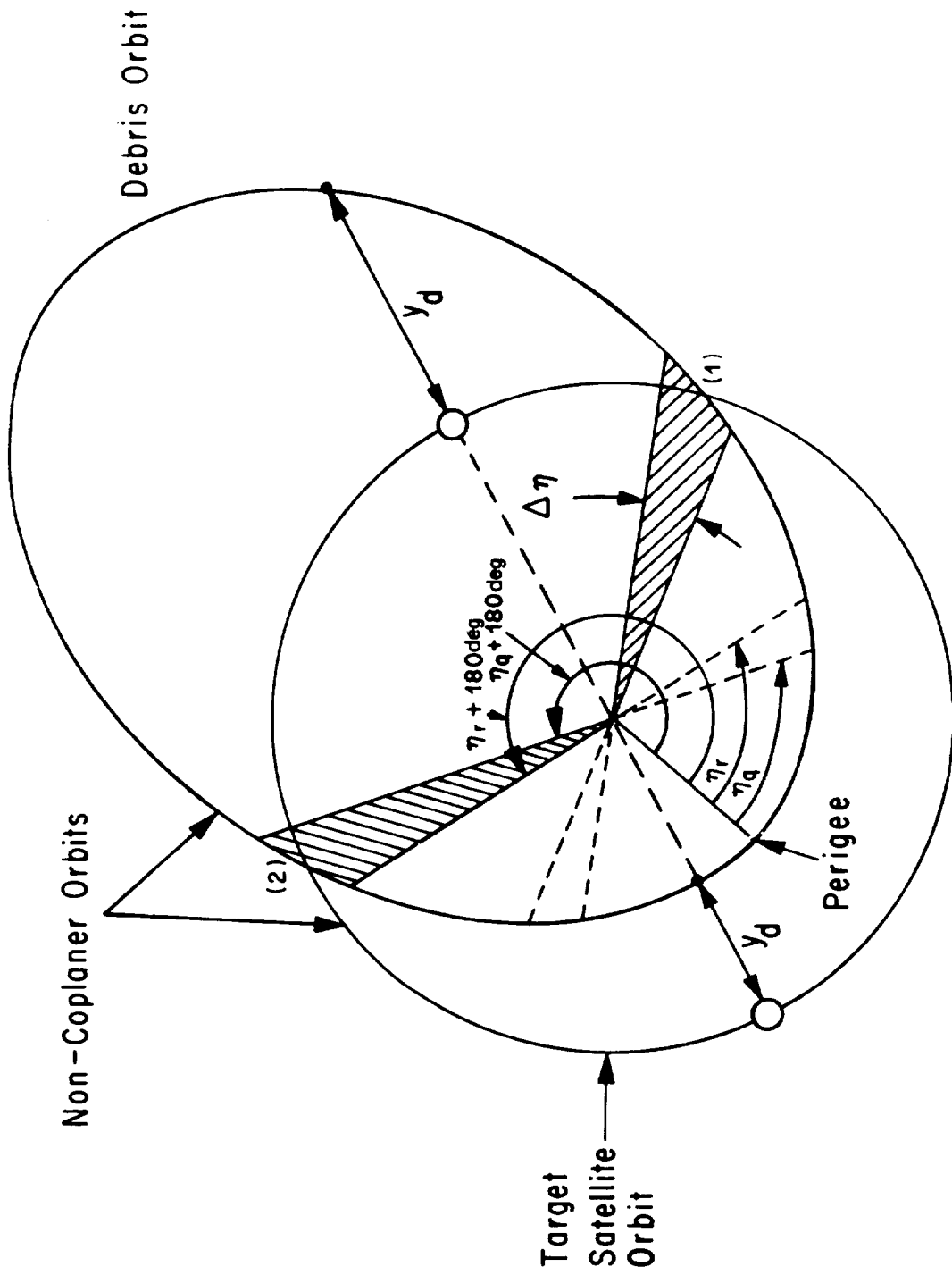


Figure 5. Positions of the orbit plane intersection line which produce collision possibilities.

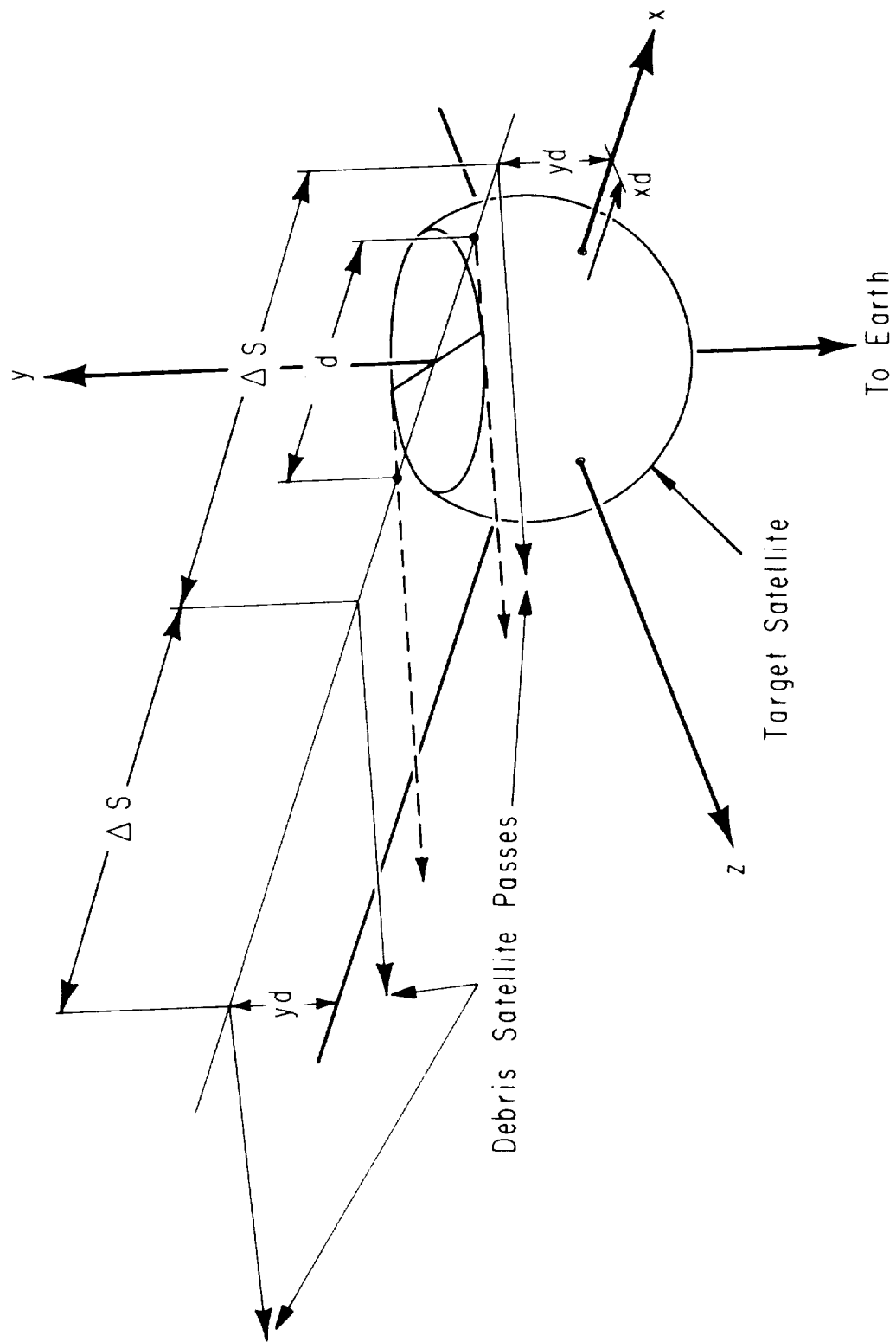


Figure 6. Geometrical description of the collision distance, d .

Equation (1) is for a Δx equal to $(1/6) \Delta S$. For any size Δx

$$m = \frac{n}{\Delta S / \Delta x} \quad . \quad (2)$$

and

$$\frac{m}{n} = \frac{\Delta x}{\Delta S} \quad . \quad (3)$$

A fundamental definition of probability is as follows: If there are n mutually exclusive, exhaustive, and equally likely cases, and m of these are favorable to an event A , then the probability of A is m/n . Since equation (3) holds for any Δx , it holds when $\Delta x = d$. By the above definition, the probability that the debris satellite will pass within the interval d is

$$P_{\text{lap}} = \frac{m}{n} = \frac{d}{\Delta S} \quad . \quad (4)$$

Since the debris satellite has a single chance to pass through the interval d each time the debris and target satellites lap each other, P_{lap} is the probability per lap.

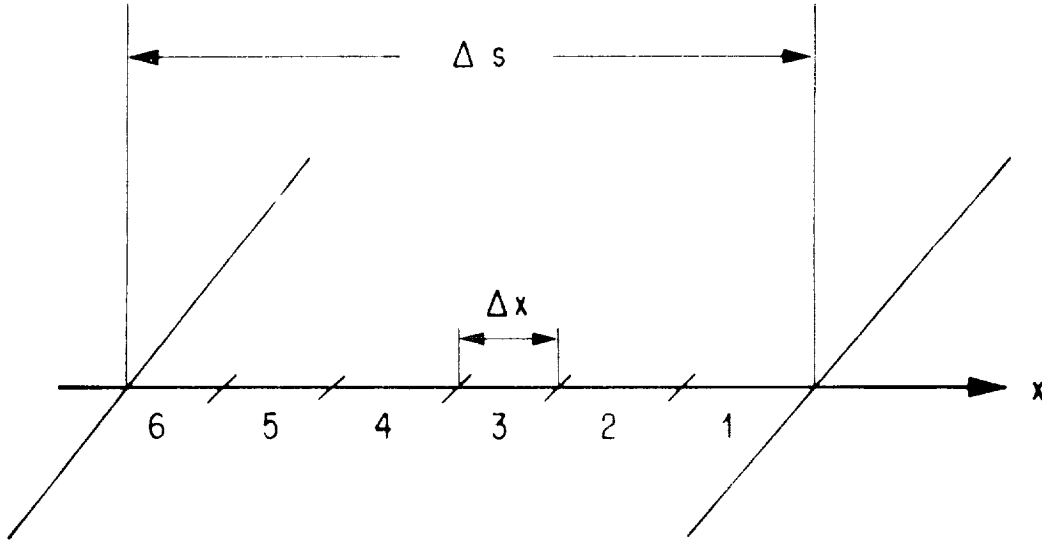


Figure 7. Geometrical explanation of collision probability expression.

Equation (4) was developed for a given mutual orbit plane orientation, (the assumption was made that inclinations, arguments of perigee, and node separation angles were known). The quantity, d , and therefore P_{lap} , is a function of these quantities. The perturbation rates (because of the earth's oblateness) of node separation and argument of perigee are great enough so that it is impractical to maintain up-to-date measurements on these quantities. Therefore, for a given time (at which it is desired to compute a collision probability), it is assumed that node separation $\Delta\Omega$ and argument of perigee ω are unknown and that all values of these angles between 0 deg and 360 deg are equally probable. Rewriting equation (4) as functions of these variables yields

$$P_{lap} = \frac{d(\omega, \Delta\Omega)}{\Delta S} \quad . \quad (5)$$

For each value of $\Delta\Omega$, only a very restricted range of values of ω will yield a non-zero value for d ; hence, for most values of ω , $P_{lap} = 0$. The average collision probability per lap over node separation and argument of perigee is

$$\bar{P}_{lap} = \frac{1}{4\pi^2} \int_0^{2\pi} \int_0^{2\pi} P_{lap} d\omega d(\Delta\Omega) \quad . \quad (6)$$

An attempt was made to perform the double integration in equation (6) analytically. Since this attempt was not successful because of the complexity of the probability expression, the expression was numerically integrated by the trapezoidal method on a digital computer. Numerically integrating equation (6) over both variables required an excessive amount of computer time because these calculations must be made for each debris satellite in earth orbit (about 2400 presently). This problem was circumvented (losing very little accuracy) by noting, after several numerically integrated runs, that the plot of probability as a function of argument of perigee, ω , manifests itself as four humps which resemble half ellipses (Fig. 8). The reason for the four humps is made clearer by referring to Figure 5. Varying the argument of perigee, ω , from 0 deg to 360 deg has the effect of varying η , the orientation of the line of intersection between the two orbit planes relative to the position of the debris satellite perigee. The sum of ω and η is the argument of latitude (measured in the debris orbit plane) which remains constant for a given $\Delta\Omega$. The shaded areas in Figure 5 are the range of intersection line positions where a non-zero collision probability exists. Each of these orientation ranges occurs twice when η (or ω) is varied from 0 deg to 360 deg when

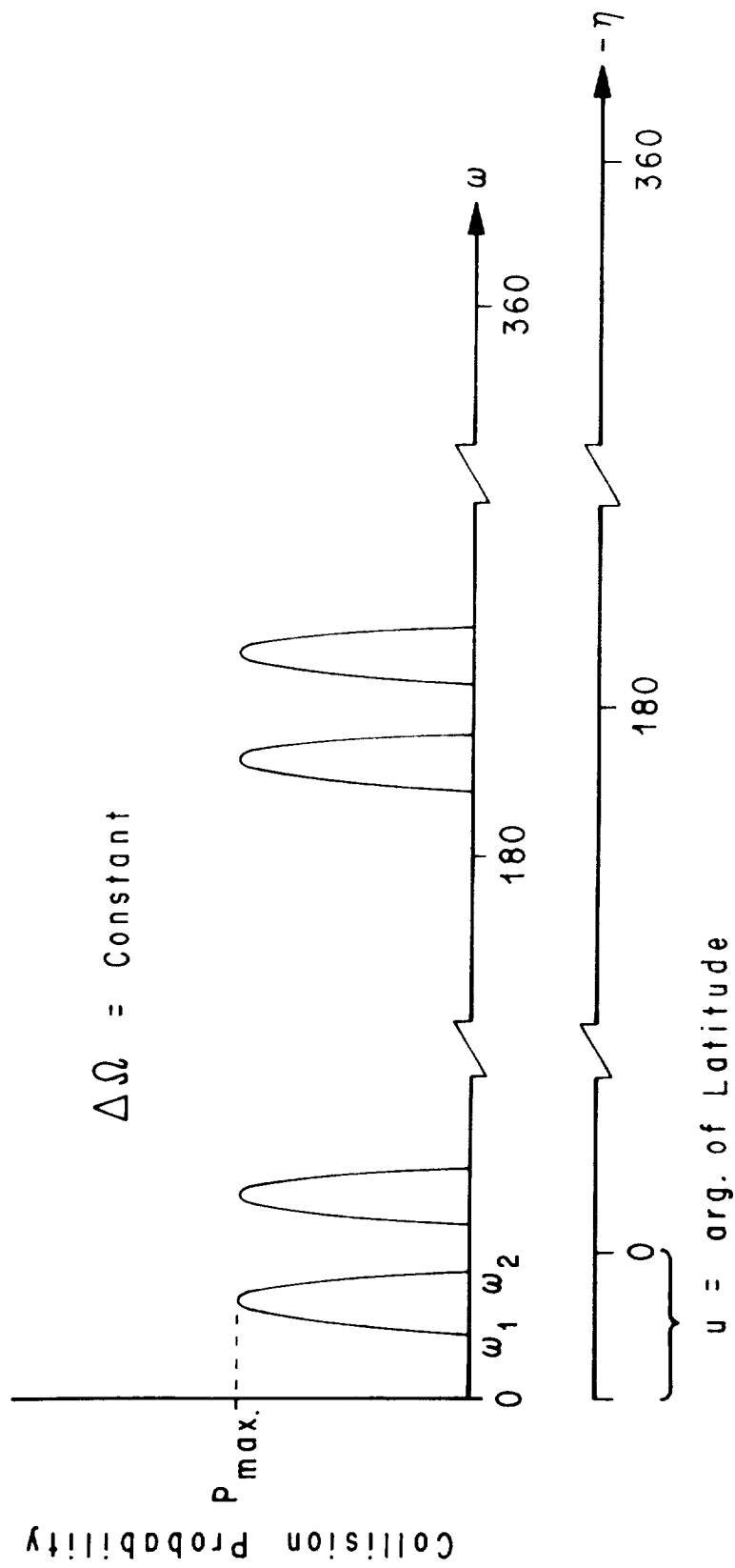


Figure 8. Illustration of typical trend in probability vs ω (or η) curve.

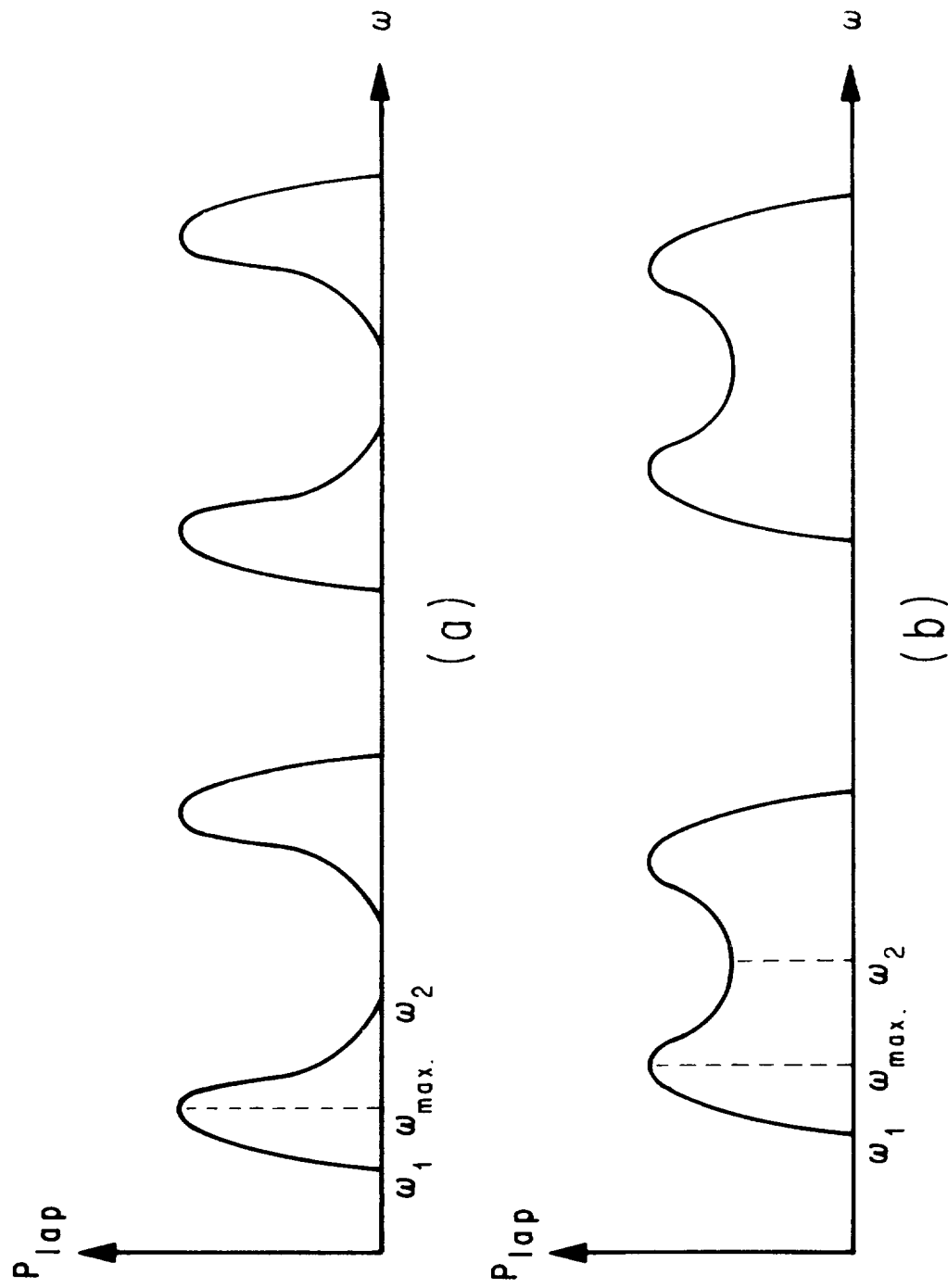


Figure 9. Trends in P_{lap} vs ω curve when apogee and/or perigee altitude of debris satellite is near target altitude

1. η is between η_q and η_r

and

2. η is between $180 + \eta_q$ and $180 + \eta_r$.

If the integral of this function (Fig. 8) is approximated as the area of two ellipses, then only the probability as a function of node separation need be numerically integrated. The method of determining the dimensions of the humps for the area calculations is described in Appendix C. A mathematical justification for the use of this ellipse approximation is given in Appendix D.

A few very special cases (debris orbits) produce a probability versus ω curve having a shape similar to the one in Figure 9 and must be numerically integrated. The elliptically shaped humps become distorted so that the area under one of the humps can no longer be approximated as the area of a half ellipse. These types of curves are generated when either the apogee or perigee of a debris satellite orbit is very near (within a few diameters of the target sphere) to the altitude of the target satellite. The humps are actually connected as in Figure 9-b when the altitude of apogee or perigee falls within the radius of the target sphere. Cases like these for which the elliptical approximation does not hold are numerically integrated over argument of perigee. Very little additional computer time is required since only a few (usually less than 10) cases like these are encountered for any given target satellite altitude.

The probability that the debris satellite (the j th satellite) will collide with the target satellite at least once within any duration mission (P_m) can be calculated once the probability for each lap in the mission, $[\bar{P}_{lap}$ (equation 6)] is known by using the following equation:

$$P_{m_j} = 1 - (1 - \bar{P}_{lap})^L, \quad (7)$$

where

L = the total number of laps that occur between the target satellite and the debris satellite.

The probability that the target satellite will collide with any one of the debris satellites is

$$P_{TOT} = 1 - \prod_{j=1}^k (1 - \bar{P}_{m_j}) \quad ,$$

where

k = the total number of debris satellites in earth orbit.

Equations (7) and (8) are derived in Appendices E and F, respectively.

SAMPLE PROBLEM

The problem of collision with debris satellites takes on special significance for the proposed modular Space Station because the expected mission duration of 10 yr and the large Space Station dimensions provide much greater exposure. An analysis of the collision hazard of the Space Station is included to illustrate the use of the computational technique and to provide additional insight into the collision problem.

The launch and operation of the modular Space Station are still some years away. The satellite population in existence at the time the mission is in progress will obviously determine the collision probability. However, future satellite populations are difficult to predict since the satellite launch rate depends on economic, political, and military factors. Therefore, an arbitrary launch date and a static satellite population were assumed. The satellite sample used in this analysis was the population and distribution in existence as of September 1970. This satellite sample contains only objects which are tracked by NORAD. The sample contains 1805 objects, but a collision is possible only with those objects which cross the Space Station's altitude.

RESULTS

The total collision probability was calculated for a range of Space Station altitudes from 200 km (108 n. mi.) to 1400 km (756 n. mi.) considering the entire satellite population. The results are shown in Figure 10. In generating these results, the Space Station inclination was held constant at 55 deg and the mission duration was assumed to be 10 yr.

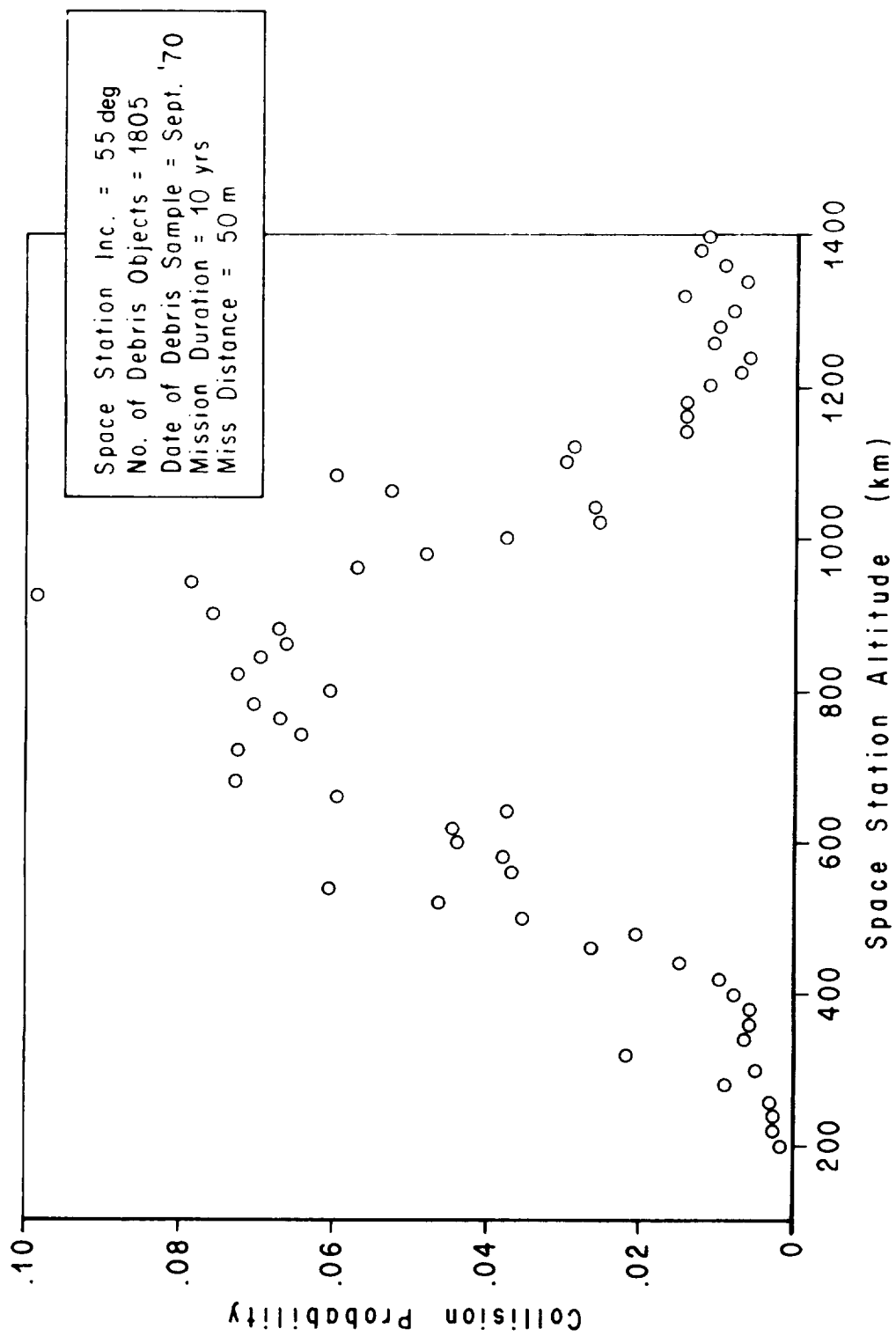


Figure 10. Total collision probability as a function of Space Station altitude.

The Space Station was represented as a sphere with a radius of 50 m. Although the actual size and configuration of the Space Station had not been finalized at the time of this study, the assumption was made, based on current design proposals, that a miss distance of 50 m from the center of the Space Station would represent either a collision or a very near miss. Therefore, the results in Figure 10 can be interpreted to be the probability that a debris satellite will intrude within a 100-m-diam sphere at least once during a 10-yr mission. A more detailed plot of the same data is given in Figure 11. In this figure the number of debris objects which cross the various altitudes is plotted. The general trend of the collision probability is to increase as the number of satellites increases. Figure 12 is a plot of collision probability versus Space Station inclination. The altitude of the Space Station was held constant at 500 km (270 n. mi.).

The collision probabilities presented in Figures 10, 11, and 12 must be regarded as minimum values, since there is considerable debris in earth orbit which is not trackable by NORAD due to the small size or the low reflectivity of the object.

A parameter study was performed to determine the types of debris orbits (size and shape) which contribute a large part to the total probability. Figure 13 shows the effect of varying perigee for constant apogee altitudes and Figure 14 is the result of varying apogee for constant perigee altitudes. The inclination of each debris orbit was held constant at 0 deg. The collision probabilities in these figures are not total probabilities but are individual satellite probabilities. These curves show that the largest contributions to the total collision probability are made by debris whose orbits are nearly circular and near the Space Station altitude. In other words, the closer the apogee or the perigee approaches the Space Station altitude, the higher the probability that a collision will occur (neglecting the effect of inclination).

Figure 15 shows an expanded view of the peak of one of the curves of Figure 13. The collision probability reaches a peak and diminishes to zero as the satellite perigee passes through the altitude band of the sphere. The same trend is also present in Figure 14 as apogee passes through the altitude band of the sphere.

Encountering some near-circular debris orbits at the various Space Station altitudes is the cause of the scattered effect in the data of Figures 10 and 11. The "spikes" in the data of Figure 12 at certain Space Station inclinations are caused by the possibility (for some nodal orientations) for the Space Station to be coplaner with the debris satellite but rotating in the opposite direction. This situation manifests itself in equation (4) as an unusually large value for d .

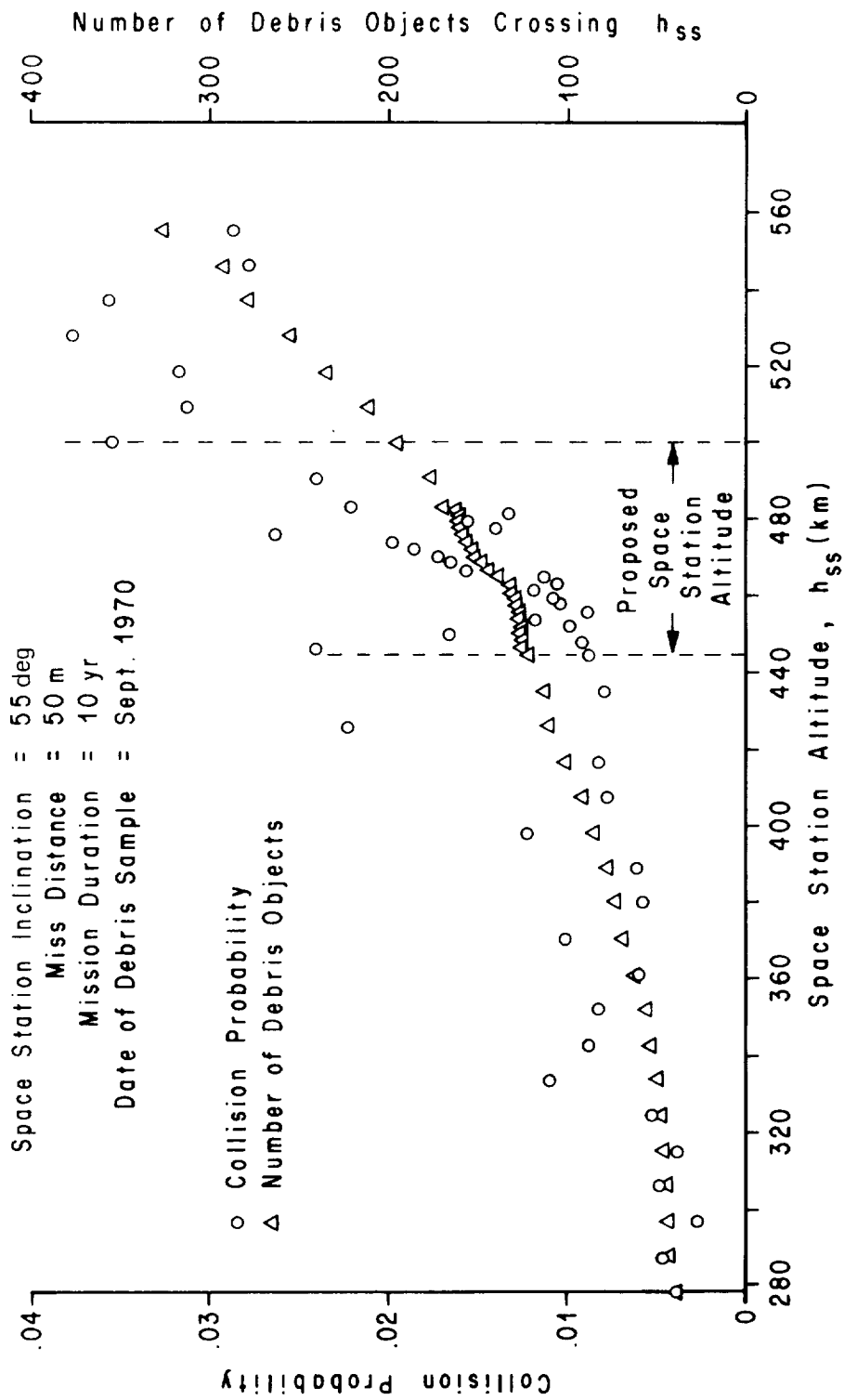


Figure 11. Total collision probability as a function of Space Station altitude, h_{ss} and the number of debris objects which cross h_{ss} .

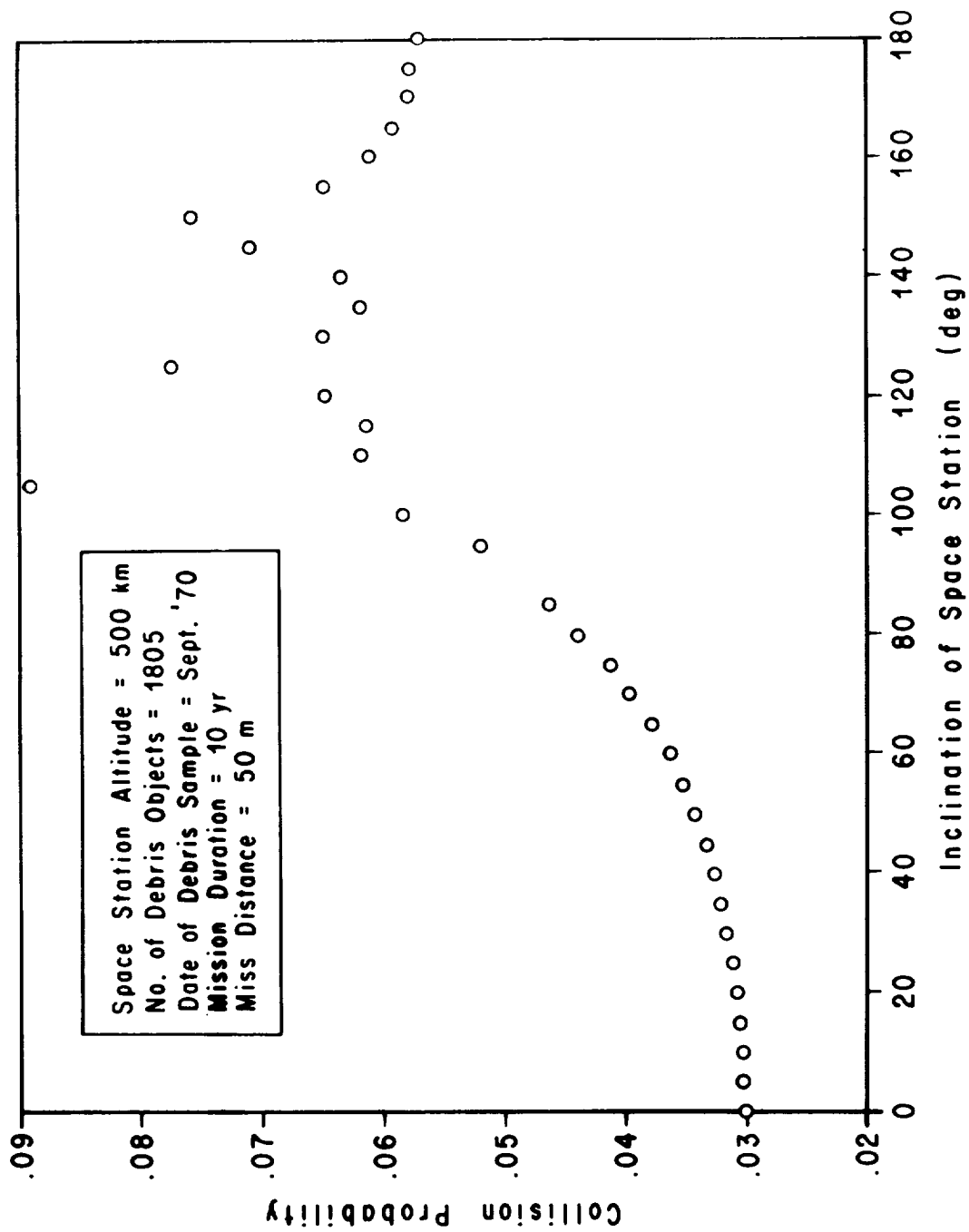


Figure 12. Total collision probability as a function of Space Station orbit inclination.

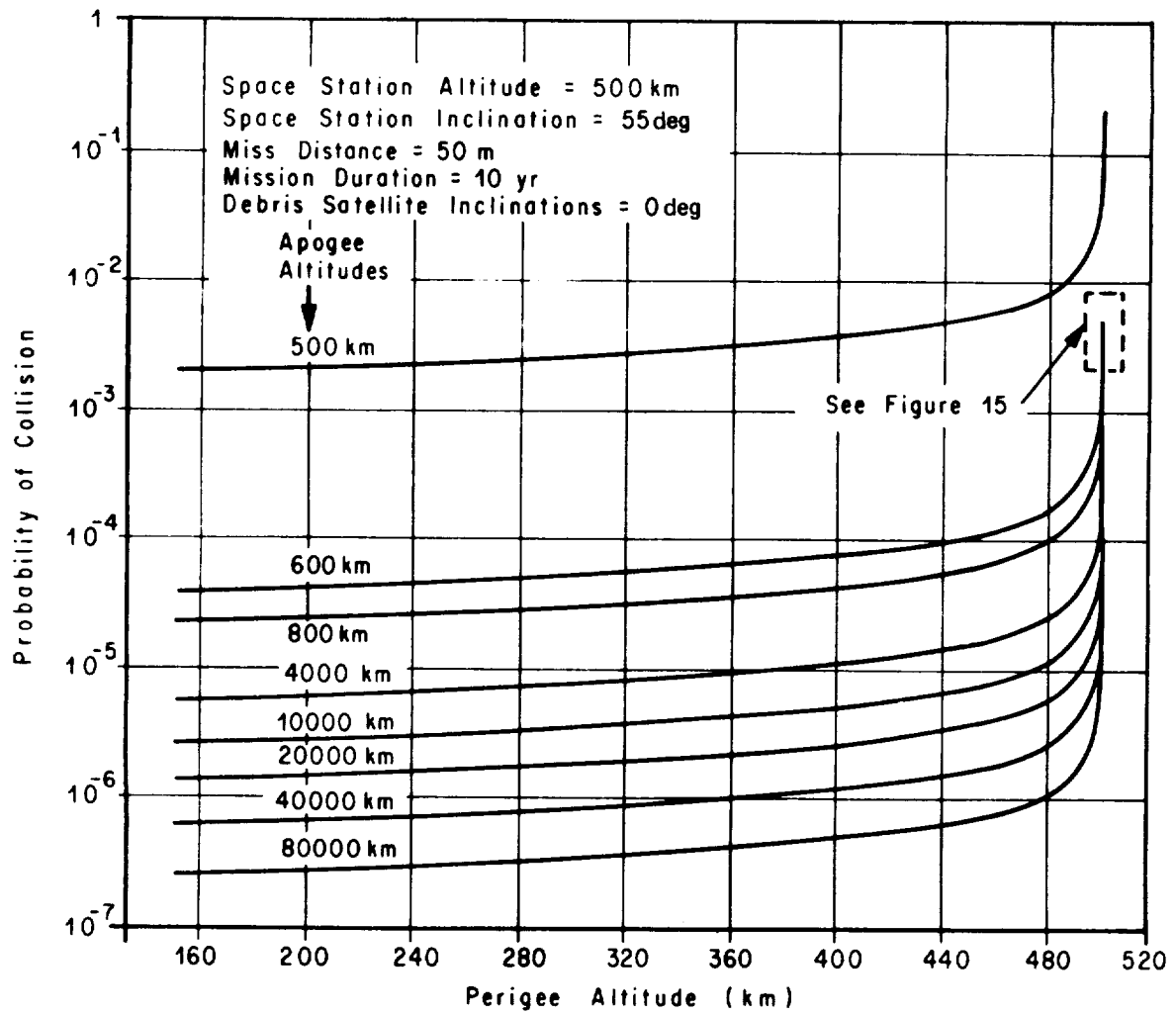


Figure 13. Probability of collision with individual debris objects as a function of perigee altitude of the debris orbit.

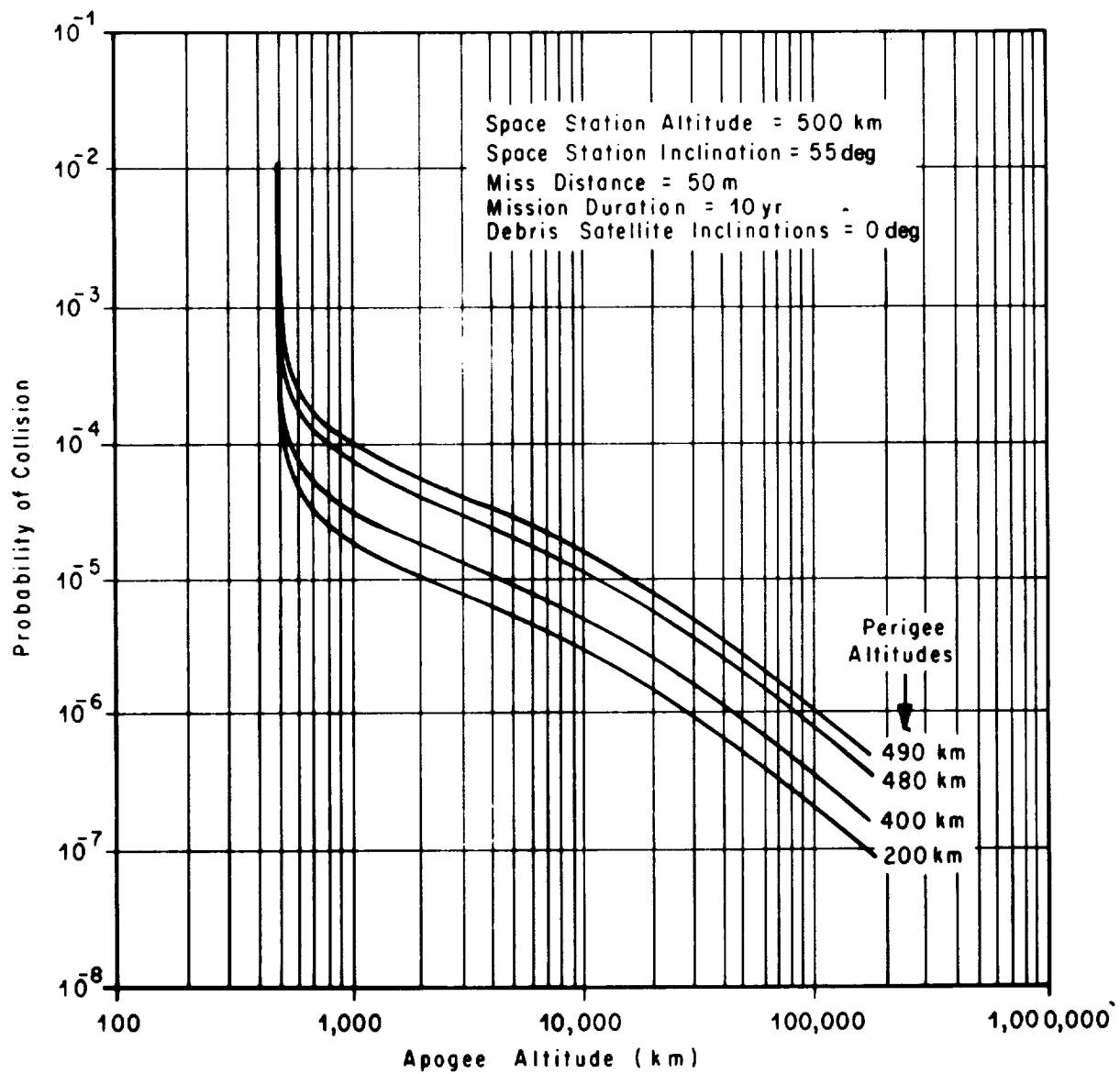


Figure 14. Probability of collision with individual debris objects as a function of apogee altitude of the debris orbit.

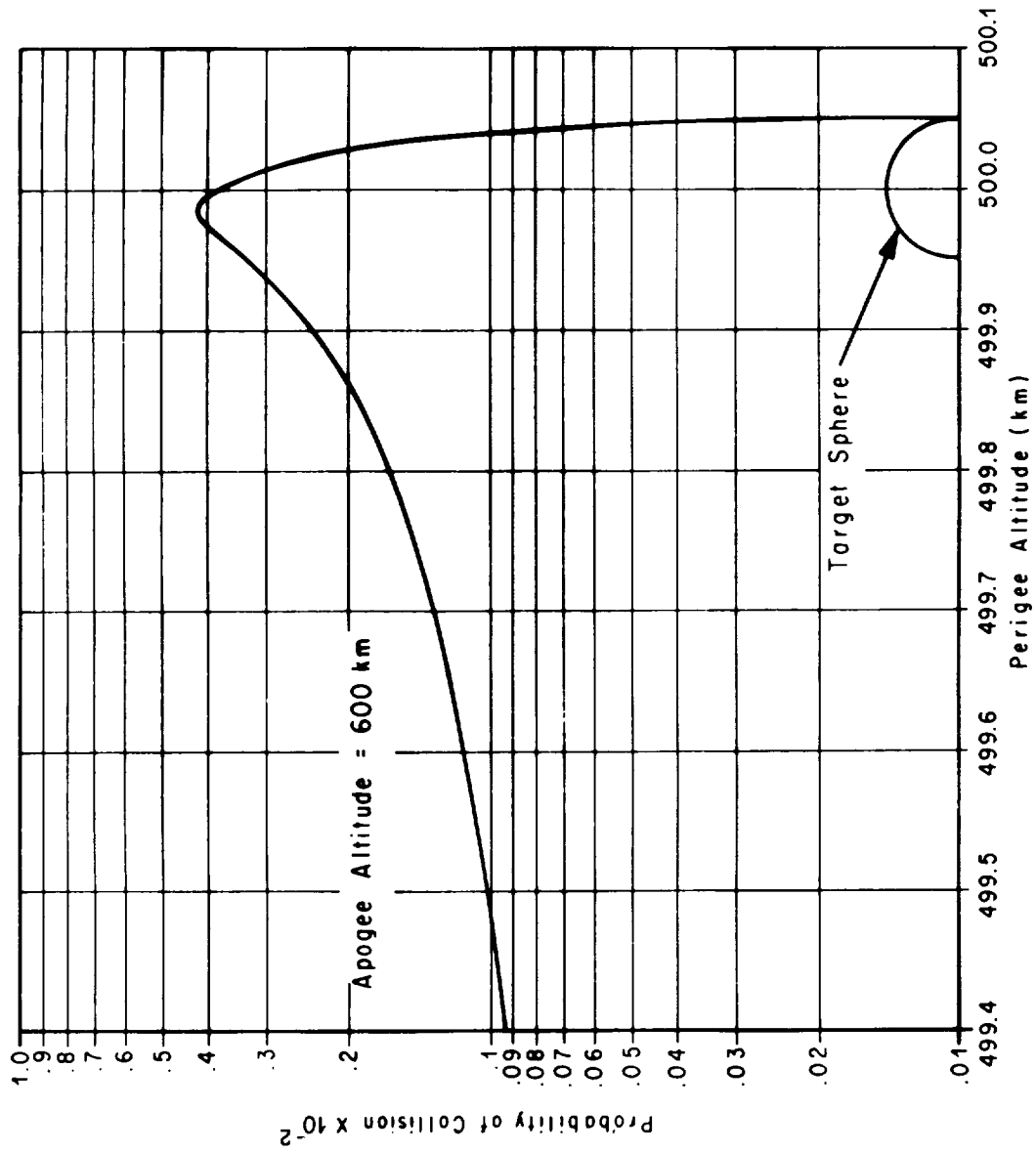


Figure 15. Variation of collision probability for an individual debris object as perigee altitude is varied through the target altitude.

The effect of the out-of-plane angle, δ , on the collision probability is illustrated in figures 16 and 17 for a few typical debris orbits. These curves show that the collision probability is greatest when the debris orbit is coplaner with the target orbit. As δ approaches zero degree a somewhat abrupt increase in collision probability occurs compared to a gradual increase as δ approaches 180 deg (retrograde coplaner orbits). The major reason for this trend is the orientation of the relative velocity vector as a function of δ . In general, high probabilities result when the relative velocity vector (and thus the trajectory of the debris object) is almost parallel to the direction of travel of the target satellite; that is, when its direction cosine is a maximum. Since the inertial velocities of the two objects are generally of the same order of magnitude, a small change in δ from zero degree immediately causes the relative velocity vector (roughly $\bar{V}_d - \bar{V}_t$) to assume a large angle with the path of the target vehicle. This acute angle gradually decreases as δ varies to 180 deg (the retrograde position) where the relative velocity vector is again nearly parallel to the direction of travel of the target vehicle.

The collision probability was parameterized over miss distance (Fig. 18) and mission duration (Fig. 19). These curves emphasize that using large vehicles in earth orbital missions of long duration result in high collision probabilities. In Figure 18, the linearity and slope of the logarithmic plot at lower probabilities (less than 0.5) show that the collision probability is approximately proportional to the square of the miss distance. For example, if the miss distance is doubled from 50 m to 100 m, the collision probability is increased approximately four times. This curve indicates that it is almost a certainty that a trackable object will pass within 1/2 km of the Space Station at least once during the 10-yr mission. Figure 19 shows that the collision probability is linear with mission duration. The circled point on Figures 18 and 19 represents the proposed Space Station mission.

CONCLUSIONS

If the present trend in satellite population growth continues, the collision hazard to men and equipment in earth orbit will become more and more severe. It seems inevitable that eventually the development and utilization of a collision avoidance system will become mandatory. Indeed, collision probabilities for the proposed modular Space Station of 0.01 to 0.04 (for the altitudes being considered) may indicate an immediate need for such a system. Some alternatives (or additions) to the above remedy are (1) stricter controls

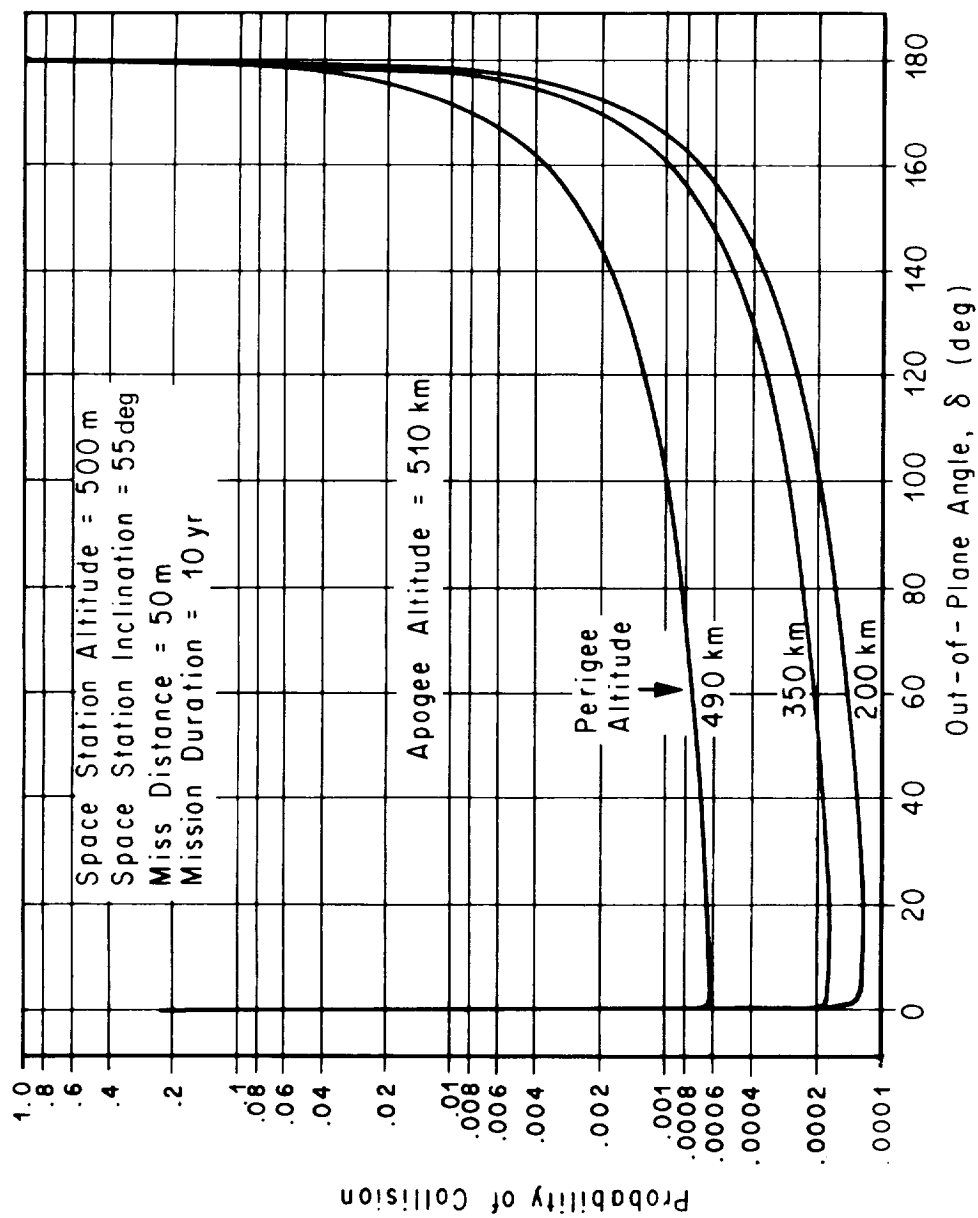


Figure 16. Effect of the out-of-plane angle, δ , on collision probability for some typical debris orbits holding apogee altitude constant.

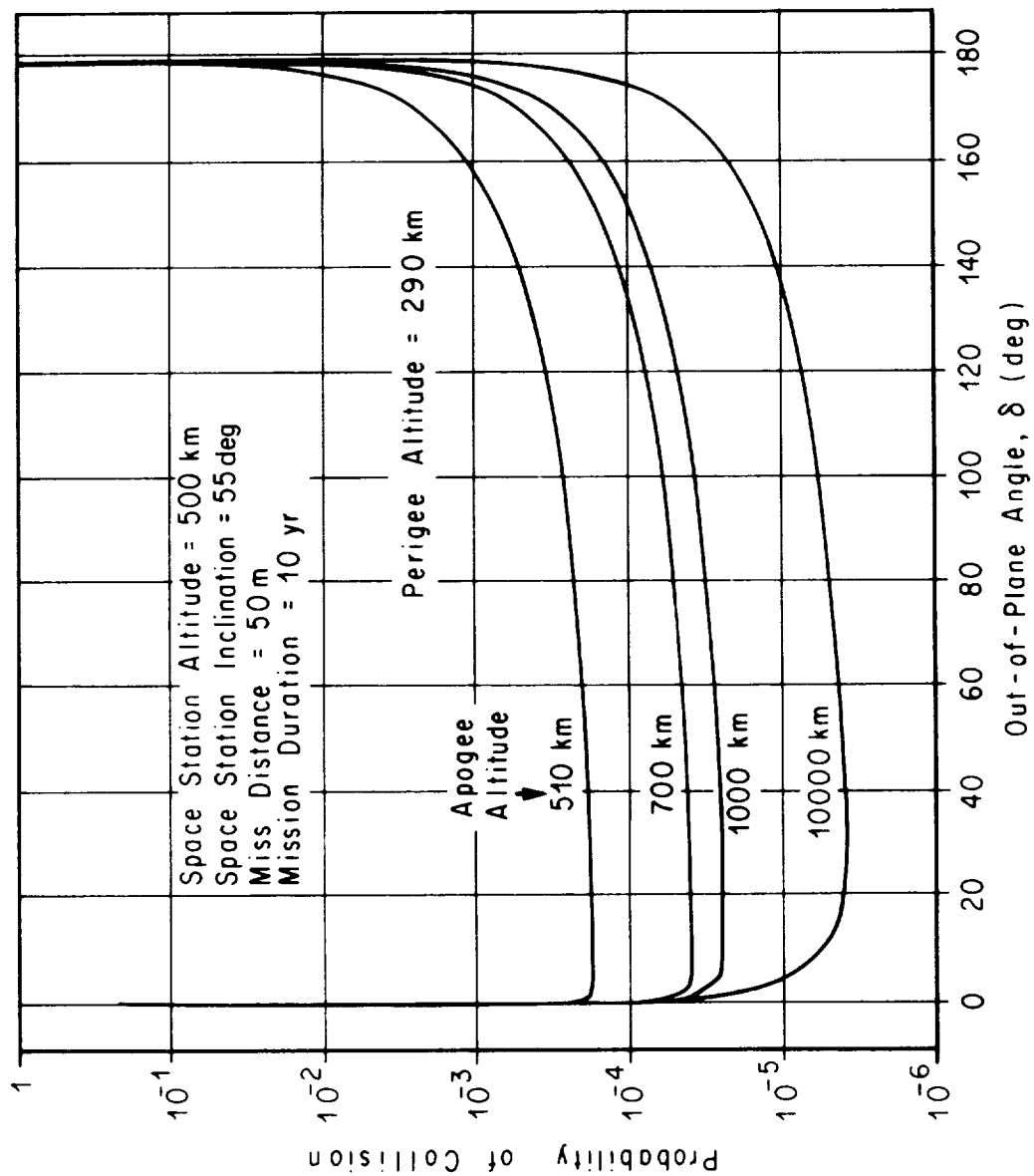


Figure 17. Effect of the out-of-plane angle, δ , on collision probability for some typical debris orbits holding perigee altitude constant.

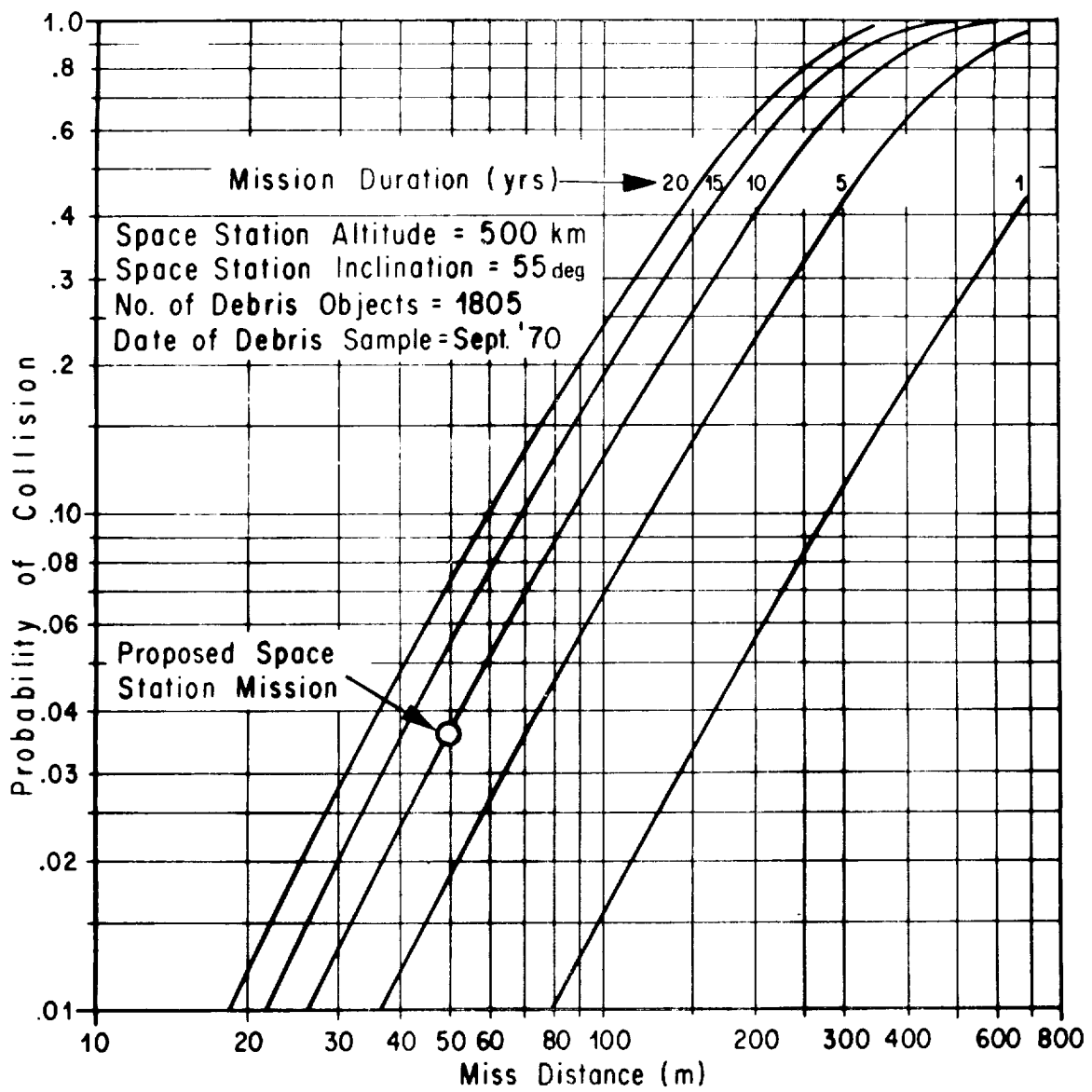


Figure 18. Total collision probability for Space Station as a function of miss distance (target sphere radius).

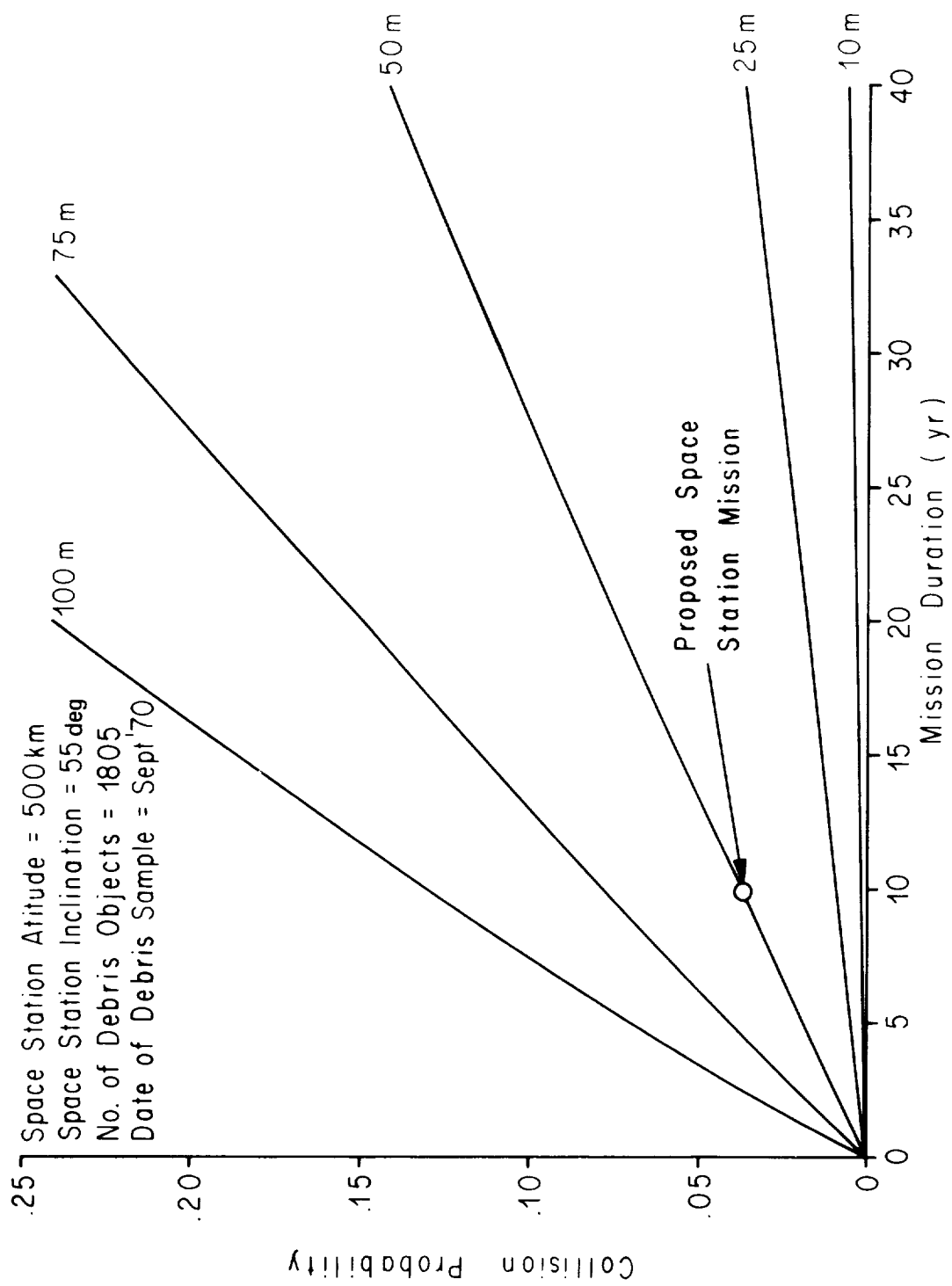


Figure 19. Total collision probability for Space Station as a function of mission duration.

on the amount of debris placed in orbit from a single launch, (2) the reservation of certain altitudes for manned vehicles or other satellites requiring collision protection, and (3) restrictions on the rate of launching objects into earth orbits (nationally and internationally).

APPENDIX A

DERIVATION OF RELATIVE VELOCITY COMPONENTS \dot{X} , \dot{Y} , \dot{Z} AND ORIENTATION ANGLES OF DEBRIS PATH θ AND β

Suppose the origin of a nonrotating right-handed system of axes is placed at the center of the earth and is defined to be an inertial reference frame. The origin of the relative coordinate system (Fig. 2) moves at a velocity (with respect to the inertial frame) equal to the velocity of the target sphere (\overline{V}_t). The immediate objective is to transform the inertial velocity vector of the debris satellite into the moving coordinate system.

The x-axis of the relative coordinate system was specified in the text as being a curvilinear axis along the path of the target vehicle. To simplify the vector transformation, the curvilinear system can be replaced by a rectangular Cartesian coordinate system where the y and z axes remain the same but the x-axis is tangent to the path of the target satellite. This allows the use of the standard transformation between two rectangular Cartesian coordinate systems, one fixed and one moving. Very little accuracy is sacrificed by doing this since computations of the relative velocity components are required only in the vicinity where a collision is possible, that is, near the origin (within the interval $-\frac{d}{z} \leq x \leq \frac{d}{z}$) of the relative coordinate system. Under this constraint, the difference between the Cartesian system and the curvilinear system is negligible.

By using the standard transformation between the two coordinate systems, the velocity of the debris satellite in the inertial system can be written as

$$\overline{V}_d = \overline{V}_r + \overline{V}_t + \overline{\omega}_t \times \overline{\rho} \quad (A-1)$$

where

\overline{V}_r = the velocity of the debris object in the relative coordinate system.

$\overline{\rho}$ = the position vector of the debris object in the relative coordinate system.

$\overline{\omega}_t$ = the rate of rotation of the relative axes with respect to the inertial system.

The required vector is \overline{V}_r . Solving equation (A-1) for this vector yields

$$\bar{\mathbf{V}}_r = \bar{\mathbf{V}}_d - \bar{\mathbf{V}}_t - \bar{\boldsymbol{\omega}}_t \times \bar{\boldsymbol{\rho}} \quad . \quad (\text{A-2})$$

Writing this equation in matrix form in terms of the three-dimensional components of each term results in

$$\begin{bmatrix} \dot{x} \\ \dot{y} \\ \dot{z} \end{bmatrix} = \begin{bmatrix} \dot{x}_d \\ \dot{y}_d \\ \dot{z}_d \end{bmatrix} - \begin{bmatrix} \dot{x}_t \\ \dot{y}_t \\ \dot{z}_t \end{bmatrix} - \begin{bmatrix} \omega_x \\ \omega_y \\ \omega_z \end{bmatrix} \times \begin{bmatrix} \rho_x \\ \rho_y \\ \rho_z \end{bmatrix} \quad . \quad (\text{A-3})$$

Figure A-1 shows the orientation of the inertial velocity vector of the debris object in terms of the flight path angle, γ , and the angle between the debris and target orbit planes, δ (δ is derived in Appendix G). Resolving this vector into its components in the directions of the relative coordinate axes yields

$$\begin{aligned} \dot{x}_d &= -V_d \cos \gamma \cos \delta \\ \dot{y}_d &= V_d \sin \gamma \\ \dot{z}_d &= V_d \cos \gamma \sin \delta \quad . \end{aligned} \quad (\text{A-4})$$

Since $\bar{\mathbf{V}}_t$ remains along the x-axis of the relative coordinate system, its three components are

$$\begin{aligned} \dot{x}_t &= -V_t \\ \dot{y}_t &= 0 \\ \dot{z}_t &= 0 \quad . \end{aligned} \quad (\text{A-5})$$

Because of the way the relative coordinate system was defined (p. 4 - second paragraph) it undergoes rotation about the z-axis only. Therefore,

$$\begin{aligned} \omega_x &= 0 \\ \omega_y &= 0 \\ \omega_z &= \omega_t \quad . \end{aligned} \quad (\text{A-6})$$

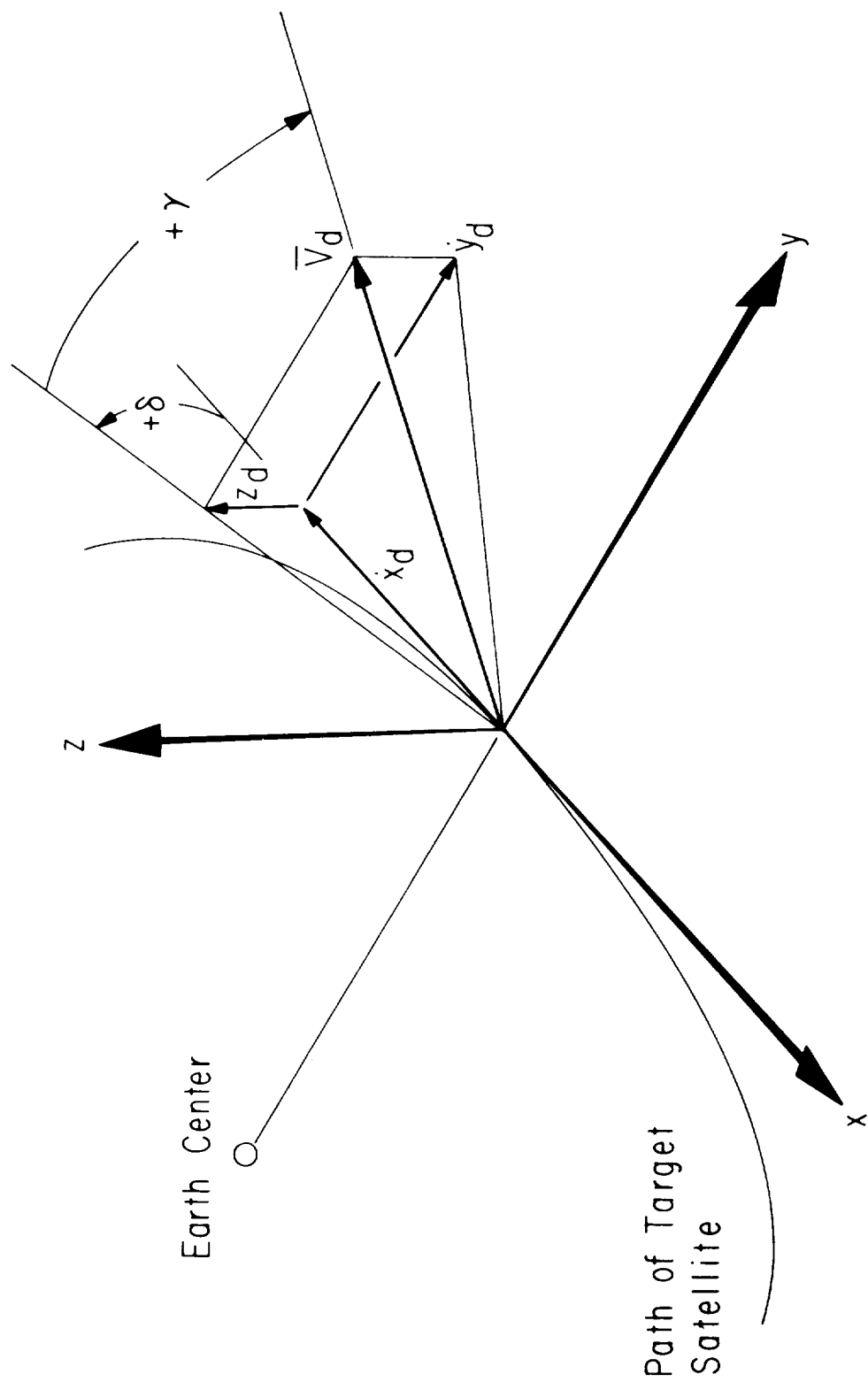


Figure A-1. Inertial velocity of the debris satellite.

The rotational rate ω_t is computed as

$$\omega_t = \frac{2\pi}{T_t} \quad ,$$

where

T_t = the orbital period of the target satellite.

The relative velocity components of the debris satellite are computed only when the debris satellite passes through the orbit plane of the target satellite. Therefore, the last matrix in equation (A-3) becomes

$$\rho_x = x_d \quad (A-7)$$

$$\rho_y = y_d$$

$$\rho_z = 0 \quad .$$

Substituting (A-4), (A-5), (A-6), and (A-7) into (A-3) yields

$$\begin{bmatrix} \dot{x} \\ \dot{y} \\ \dot{z} \end{bmatrix} = \begin{bmatrix} -V_d \cos \gamma \cos \delta \\ V_d \sin \gamma \\ V_d \cos \gamma \sin \delta \end{bmatrix} - \begin{bmatrix} -V_t \\ 0 \\ 0 \end{bmatrix} - \begin{bmatrix} 0 \\ 0 \\ \omega_t \end{bmatrix} \times \begin{bmatrix} x_d \\ y_d \\ 0 \end{bmatrix} \quad (A-8)$$

Carrying out the matrix operations yields the relative velocity components

$$\dot{x} = V_t - V_d \cos \gamma \cos \delta + \omega_t y_d \quad (A-9)$$

$$\dot{y} = V_d \sin \gamma - \omega_t x_d$$

$$\dot{z} = V_d \cos \gamma \sin \delta \quad .$$

The product $V_d \cos \gamma$ in the \dot{x} and \dot{z} equations can be replaced by C_1/R_d , where

$$C_1 = R_d V_d \cos \gamma \quad ,$$

is the angular momentum associated with the orbit of the debris satellite. Also \dot{y} can be written as a function of the true anomaly of the planar intersection

line by noting that \dot{y} is approximately equal to \dot{R}_d . Therefore,

$$\dot{y} = \frac{d}{dt} (R_d) = \frac{d}{dt} \left(\frac{p}{1 + e \cos \eta} \right) = \frac{ep \sin \eta \dot{\eta}}{(1 + e \cos \eta)^2} \quad . \quad (A-10)$$

Multiplying the right side of equation (A-10) by R_d^2/R_d^2 and noting that

$$C_1 = R_d^2 \dot{\eta} \quad ,$$

equation (A-10) changes to

$$\dot{y} = \frac{C_1 p e \sin \eta}{(1 + e \cos \eta)^2 R_d^2} \quad . \quad (A-11)$$

Since

$$R_d^2 = \frac{p^2}{(1 + e \cos \eta)^2}$$

equation (A-11) reduces to

$$\dot{y} = \frac{C_1 e}{p} \sin \eta \quad . \quad (A-12)$$

Since

$$p = \frac{C_1^2}{\mu} \quad ,$$

$$\dot{y} = \frac{\mu e}{C_1} \sin \eta \quad . \quad (A-13)$$

The relative velocity components are finally written as

$$\dot{x} = V_t - \frac{C_1}{R_d} \cos \delta + \omega_t y_d \quad (A-14)$$

$$\dot{y} = \frac{\mu e}{C_1} \sin \eta$$

$$\dot{z} = \frac{C_1}{R_d} \sin \delta \quad .$$

Referring to Figure A-2, the debris path orientation angles are

$$\theta = \tan^{-1} \left(\frac{\dot{z}}{\dot{x}} \right) \quad (\text{A-15})$$

and

$$\beta = \tan^{-1} \left(\frac{\dot{y}}{\dot{x}} \right) \quad .$$

Comparing equations (A-15) with equations (A-9), it is found that

$$\beta = f(x_d) \quad . \quad (\text{A-16})$$

The technique used to calculate the collision distance (Appendix B) dictates that β remain constant as x_d varies. Therefore, the $\omega_t x_d$ term in equations (A-9) (the \dot{y} equation) is considered to be zero since its value will always be small (less than 1 m/s).

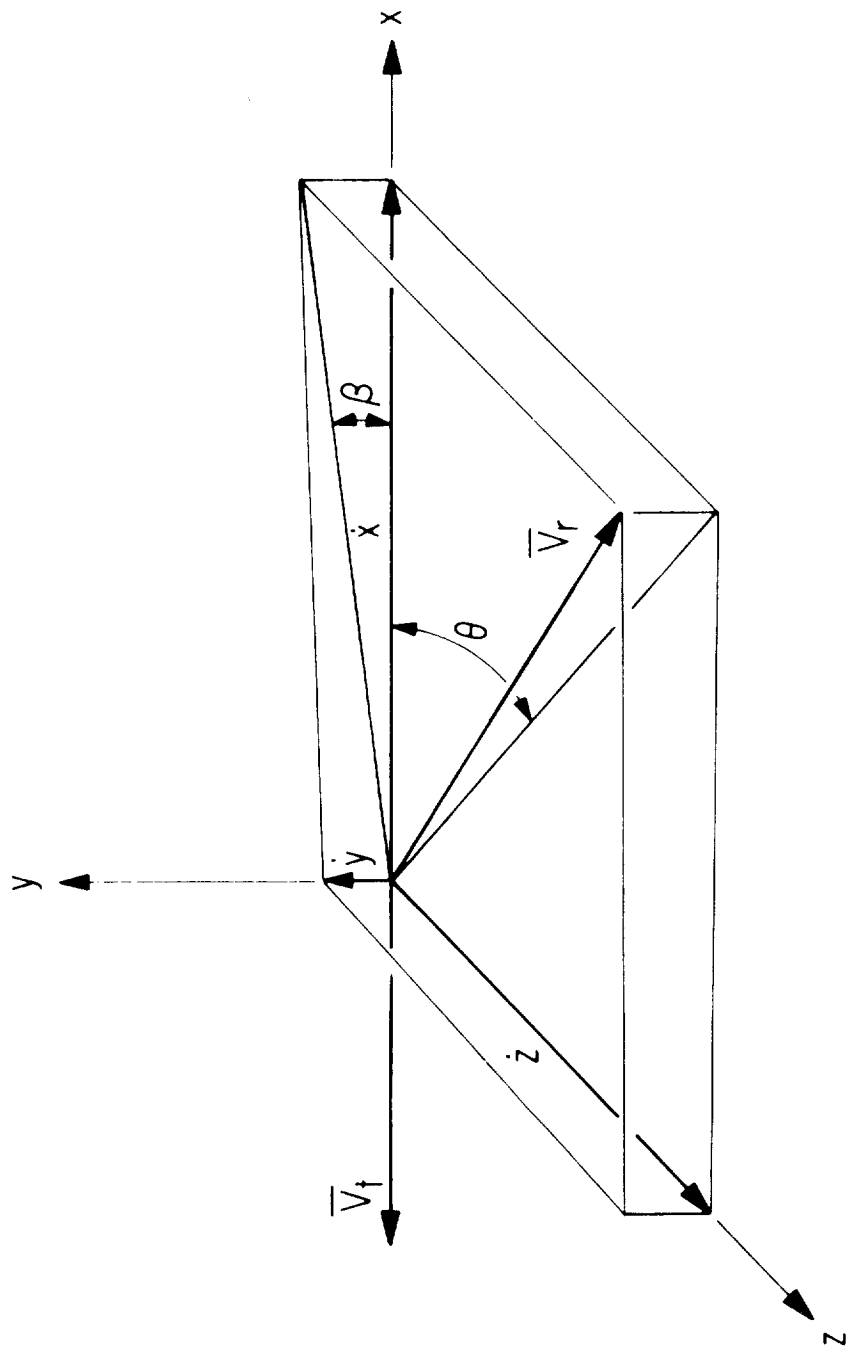


Figure A-2. Relative velocity vector, \vec{V}_r .

APPENDIX B

DERIVATION OF THE COLLISION DISTANCE, d

As stated in the text, the only varying quantity associated with successive passes of the debris satellite through the orbit plane of the target satellite is the horizontal position of the intersection point. Figure 6 shows several of these successive passes. This figure shows that if the debris satellite passes through the target orbit plane within a distance of $d/2$ from the y axis, then the debris object will intersect the sphere, thus defining a collision. The distance d is a function of the three-dimensional direction of travel of the debris object and the altitude difference at plane intersection, y_d .

In order to determine d , the equation of the target sphere is first solved simultaneously with the equations of the line of travel of the debris object. This yields the coordinates of the points at which the debris path intersects the sphere. The position of the debris intersection with the x, y plane (x_d, y_d) is then varied in the x direction to generate the range of values of x_d which produces real (mathematically) intersection points with the target sphere. The altitude difference y_d is maintained constant as are the β and θ angles defining the direction of travel. This range of values of x_d is equal to d . The derivation follows:

The equation of the sphere which represents the target satellite is

$$x^2 + y^2 + z^2 = R^2, \quad (\text{B-1})$$

where R is the miss distance (or sphere radius). The equations which specify the debris satellite trajectory, assuming that it travels in a straight line and has the same direction as the relative velocity vector in the relative coordinate system, are

$$y = (x - x_d) \tan \beta + y_d \quad (\text{B-2})$$

$$z = (x - x_d) \tan \theta \quad . \quad (\text{B-3})$$

The parameters x_d and y_d are the x and y coordinates, respectively, of the point where the debris satellite passes through the orbit plane of the target satellite. Figure 6 shows this geometrically. To find the intersection points of the debris trajectory with the target sphere, equations (B-2) and (B-3) are substituted into equations (B-1) and the terms are collected on x^2 and x , yielding

$$a_1 x^2 + b_1 x + c_1 = 0 \quad (B-4)$$

where

$$a_1 = 1 + \tan^2 \beta + \tan^2 \theta \quad (B-5)$$

$$b_1 = 2y_d \tan \beta - 2x_d (\tan^2 \beta + \tan^2 \theta)$$

$$c_1 = x_d^2 \tan^2 \beta - 2x_d y_d \tan \beta + y_d^2 + x_d^2 \tan^2 \theta - R^2$$

Solving equation (B-4) for x , the x-coordinates of the points where the line of travel cuts the sphere are obtained:

$$x = \frac{b_1}{2a_1} \pm \frac{\sqrt{b_1^2 - 4a_1 c_1}}{2a_1} \quad (B-6)$$

The y and z coordinates are given by equations (B-2) and (B-3).

In equation (B-6) above, if $b_1^2 = 4a_1 c_1$, the debris trajectory is tangent to the sphere; if $b_1^2 > 4a_1 c_1$, it intersects the sphere at two points; if $b_1^2 < 4a_1 c_1$, no intersection occurs. It is required to find the range of values of x_d which satisfy the inequality

$$b_1^2 \geq 4a_1 c_1 \quad (B-7)$$

Substituting equations (B-5) into equation (B-7) and collecting terms on x_d^2 and x_d yields

$$a_2 x_d^2 + b_2 x_d + c_2 \geq 0 \quad (B-8)$$

where

$$a_2 = -4(\tan^2\beta + \tan^2\theta) \quad (B-9)$$

$$b_2 = 8y_d \tan \beta$$

$$c_2 = 4[(R^2 - y_d^2) \sec^2\theta + R^2 \tan^2\beta]$$

The solution of the above inequality is

$$x_{d_1} \leq x_d \leq x_{d_2} \quad , \quad (B-10)$$

where

$$x_{d_1} = \frac{-b_2}{2a_2} + \frac{\sqrt{b_2^2 - 4a_2c_2}}{2a_2}$$

and

$$x_{d_2} = \frac{-b_2}{2a_2} - \frac{\sqrt{b_2^2 - 4a_2c_2}}{2a_2} \quad .$$

The collision distance, then, is

$$d' = x_{d_2} - x_{d_1} = - \frac{\sqrt{b_2^2 - 4a_2c_2}}{a_2} \quad . \quad (B-11)$$

This is the interval along the x-axis through which the debris object can pass and intersect the sphere.

APPENDIX C

AREA DETERMINATION OF PROBABILITY VERSUS ω HUMP.

To determine the dimensions of the humps in Figure 8, it is noted that the maximum probability (for each $\Delta\Omega$ increment) as a function of ω occurs when the altitudes of the two bodies are equal at the line of intersection between the orbit planes. When this occurs the value of y_d goes to zero and the cap that is cut off the sphere in Figure 7, becomes a hemisphere causing the collision distance d to reach a maximum. The true anomaly of the intersection line (measured from the line of perigee in the debris orbit) at which $\bar{R}_d = \bar{R}_t$ is calculated as

$$\eta_{\max.} = \cos^{-1} \left[\frac{p - R_t}{eR_t} \right] \quad . \quad (C-1)$$

The sum of the true anomaly, η , and the argument of perigee, ω , is the argument of latitude, u . Thus,

$$\omega_{\max.} = u - \eta_{\max.} \quad . \quad (C-2)$$

Substituting the above value of $\omega_{\max.}$ into the probability expression [equation (5) in the text] yields the maximum collision probability as

$$P_{\max.} = \frac{d(\omega_{\max.}, \Delta\Omega)}{\Delta S} \quad . \quad (C-3)$$

where

$P_{\max.}$ = the height of the probability hump of Figure 8.

To obtain the width of the hump, $\Delta\omega$, it is required to find the values of ω where the probability goes to zero. The probability expression is set equal to zero yielding

$$P_{\text{lap}} = d/\Delta S = 0$$

or

$$d = 0 \quad . \quad (C-5)$$

From Appendix B,

$$d = - \frac{\sqrt{b_2^2 - 4a_2c_2}}{a_2} \quad . \quad (C-6)$$

Therefore to satisfy equation (C-5)

$$b_2^2 - 4a_2c_2 = 0 \quad , \quad (C-7)$$

where

$$a_2 = -4(\tan^2\beta + \tan^2\theta) \quad (C-8)$$

$$b_2 = 8y_d \tan \beta$$

$$c_2 = 4[(R^2 - y_d^2) \sec^2\theta + R^2 \tan^2\beta] \quad .$$

Substituting equations (A-15) and (C-8) into (C-7) and solving for the altitude difference, y_d , yields

$$y_{d1} = + R \sqrt{\frac{\dot{y}^2 + \dot{z}^2}{\dot{z}^2}} \quad \text{and} \quad y_{d2} = -R \sqrt{\frac{\dot{y}^2 + \dot{z}^2}{\dot{z}^2}} \quad (C-9)$$

where \dot{y} and \dot{z} are derived in Appendix A. The quantities y_{d1} and y_{d2} are the altitude differences between the two bodies where the collision probability goes to zero. These two values are then used to calculate the orbital radius of the debris satellite (at the line of intersection between the orbit planes) at which the collision probability goes to zero as

$$R_{d1,2} = R_t + y_{d1,2} \quad . \quad (C-10)$$

The position (true anomaly) in the orbit of the debris satellite where this radius occurs is

$$\eta_{1,2} = \cos^{-1} \left[\frac{p - R_{d1,2}}{e R_{d1,2}} \right] \quad , \quad (C-11)$$

where

p = the semilatus rectum

e = the eccentricity.

The arguments of perigee corresponding to η_1 and η_2 are expressed as

$$\omega_{1,2} = u - \eta_{1,2} \quad , \quad (C-12)$$

where

u = the argument of latitude (in the debris orbit) of the intersection line.

The difference between ω_1 and ω_2 is the width of the probability versus ω hump. Thus,

$$\Delta\omega = \omega_2 - \omega_1 = (u - \eta_2) - (u - \eta_1)$$

or

$$\Delta\omega = \eta_1 - \eta_2 \quad . \quad (C-13)$$

$\Delta\omega$ is typically less than .5 deg for a miss distance of 50 m. The area of the probability versus ω hump is then approximated as one-half of an ellipse with the minor axis equal to $\Delta\omega$ and the major axis equal to $2 P_{\max.}$.

(Appendix D for justification). The approximate area of one hump is

$$A = \frac{1}{4} \pi P_{\max.} \Delta\omega \quad . \quad (C-14)$$

APPENDIX D

MATHEMATICAL JUSTIFICATION FOR ELLIPTICAL APPROXIMATION OF INTEGRAL

Figure D-1 shows the target sphere and the two positions at which the debris path can be tangent to the sphere. These two tangent points lie on a small circle of the sphere. An edgewise view of this circle is shown in Figure D-2 as seen by an observer looking down the x-axis in the +x direction. The plane of this circle is always perpendicular to the y-z plane since y_d , θ , and β remain constant for successive passes of the debris satellite through the target orbit plane and the only variable is x_d . In figure D-2, the radius of the small circle is r and

$$r^2 = R^2 - (y_d \cos \alpha)^2 \quad . \quad (D-1)$$

Since

$$\alpha = \tan^{-1} \left(\frac{\dot{y}}{\dot{z}} \right) \quad ,$$

then

$$\cos \alpha = \frac{\dot{z}}{\sqrt{\dot{y}^2 + \dot{z}^2}} \quad .$$

Equation (D-1) can then be written

$$r^2 = R^2 - y_d^2 \left(\frac{\dot{z}^2}{\dot{y}^2 + \dot{z}^2} \right) \quad . \quad (D-2)$$

From Figure D-1, d can be related to r in terms of the relative velocity components by taking the dot product of \bar{V}_r and \bar{i} , a unit vector in the x-direction, as follows:

$$\bar{V}_r \cdot \bar{i} = V_r \cos \epsilon = \dot{x} \quad . \quad (D-3)$$

Therefore

$$\cos \epsilon = \frac{\dot{x}}{V_r} \quad . \quad (D-4)$$

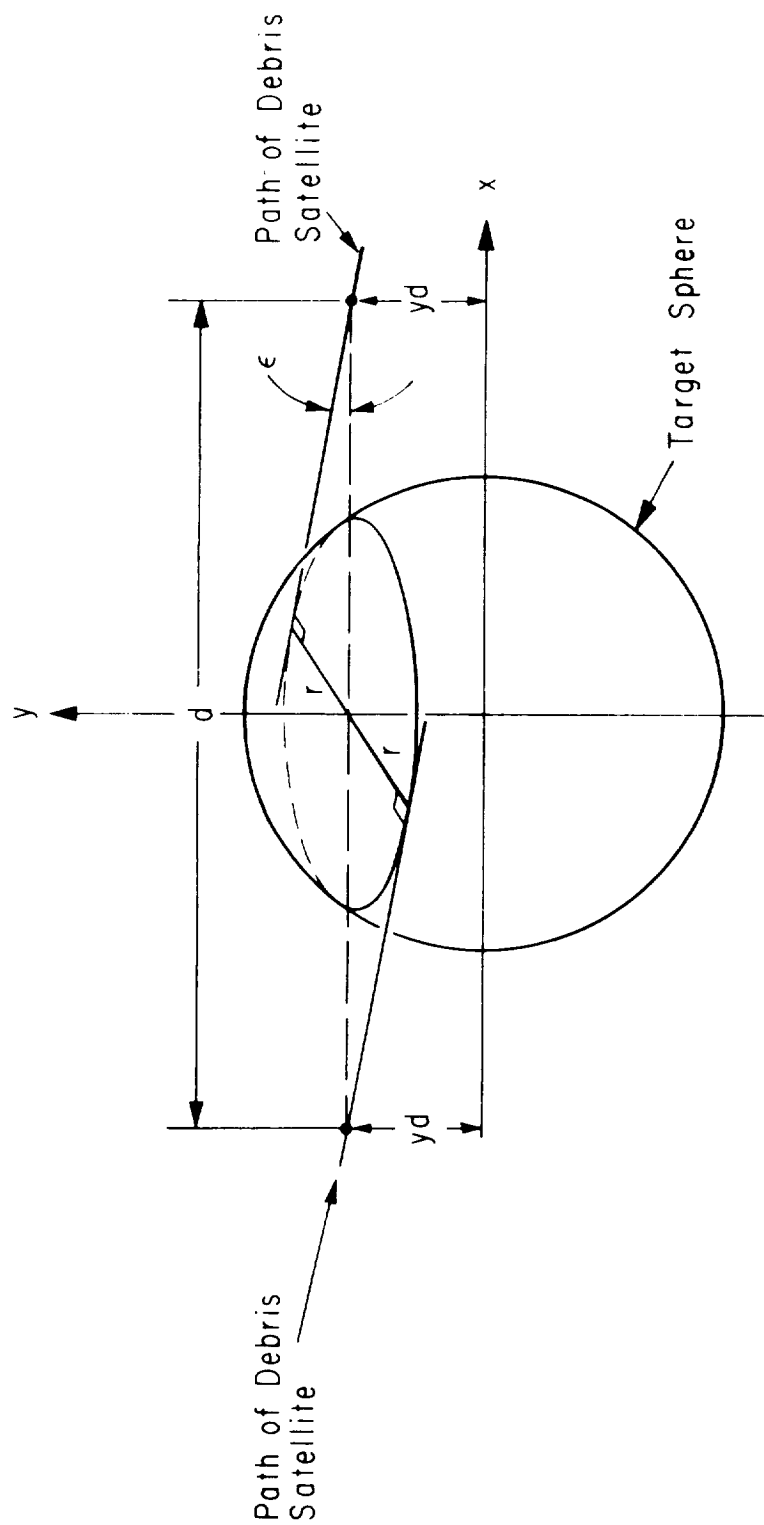


Figure D-1. Geometrical description of the collision distance, d .

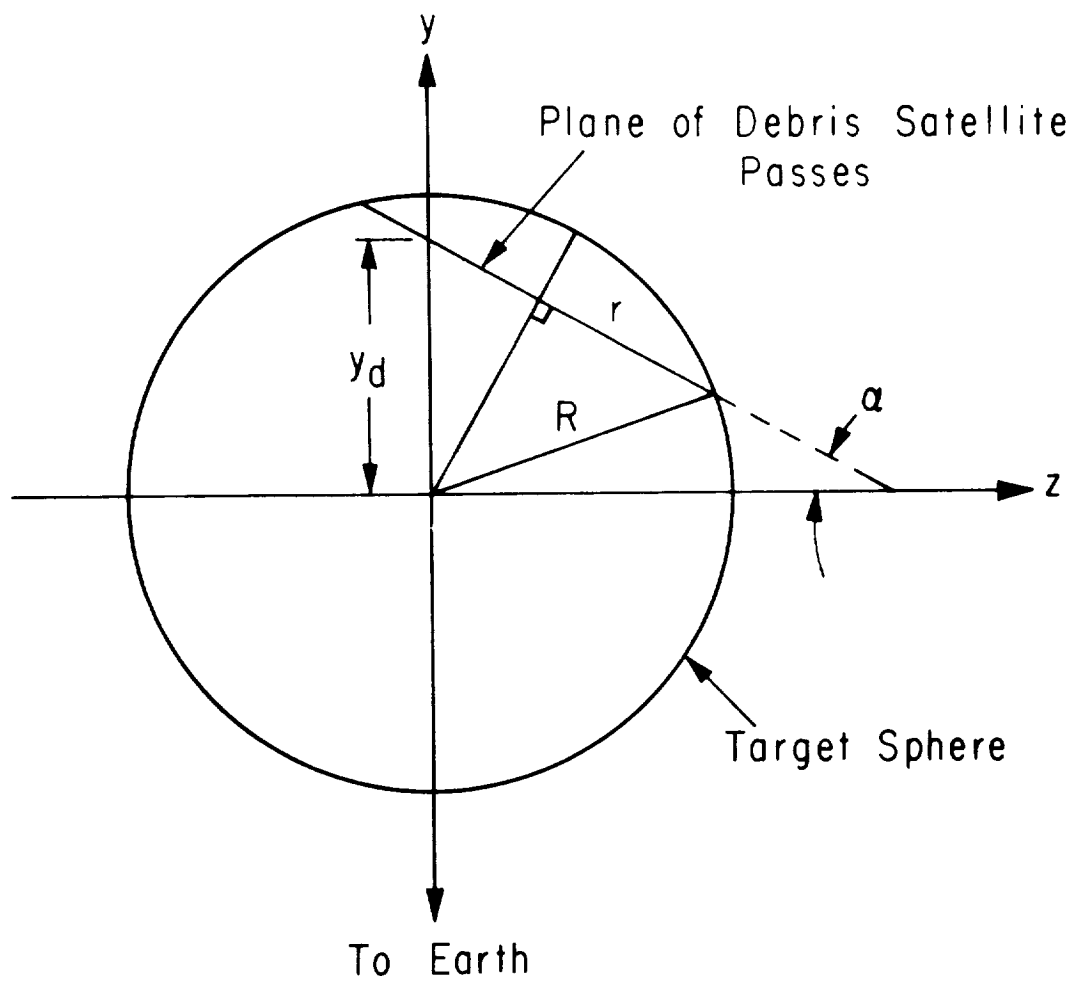


Figure D-2. Edgewise view of the small circle in the target sphere defined by passage of the debris object through the target sphere.

Squaring equation (D-4) and substituting it into the trigonometric identity

$$\sin^2 \epsilon = 1 - \cos^2 \epsilon \quad (\text{D-5})$$

yields

$$\begin{aligned} \sin^2 \epsilon &= 1 - \frac{\dot{x}^2}{V_r^2} \\ &= \frac{\dot{y}^2 + \dot{z}^2}{V_r^2} \\ &= \frac{\dot{y}^2 + \dot{z}^2}{\dot{x}^2 + \dot{y}^2 + \dot{z}^2} \quad . \end{aligned} \quad (\text{D-6})$$

From Figure D-1

$$\sin \epsilon = \frac{2r}{d} \quad . \quad (\text{D-7})$$

Squaring equation (D-7), substituting equation (D-6), and solving for d^2 results in

$$d^2 = 4r^2 \left[\frac{\dot{x}^2 + \dot{y}^2 + \dot{z}^2}{\dot{y}^2 + \dot{z}^2} \right] \quad . \quad (\text{D-8})$$

Substituting (D-2) into (D-8) gives

$$d^2 = 4 \left[R^2 - y_d^2 \left(\frac{\dot{z}^2}{\dot{y}^2 + \dot{z}^2} \right) \right] \left[\frac{\dot{x}^2 + \dot{y}^2 + \dot{z}^2}{\dot{y}^2 + \dot{z}^2} \right] \quad . \quad (\text{D-9})$$

Carrying out the multiplication yields

$$d^2 = 4R^2 \frac{(\dot{x}^2 + \dot{y}^2 + \dot{z}^2)}{\dot{y}^2 + \dot{z}^2} - \frac{4\dot{z}^2 (\dot{x}^2 + \dot{y}^2 + \dot{z}^2)}{(\dot{y}^2 + \dot{z}^2)^2} y_d^2$$

and upon rearranging,

$$d^2 + \frac{4\dot{z}^2(\dot{x}^2 + \dot{y}^2 + \dot{z}^2)}{(\dot{y}^2 + \dot{z}^2)^2} y_d^2 = \frac{4R^2(\dot{x}^2 + \dot{y}^2 + \dot{z}^2)}{\dot{y}^2 + \dot{z}^2} \quad . \quad (\text{D-10})$$

Both sides of equation (D-10) are divided by the right side to give

$$\frac{d^2}{4R^2 \left[\frac{\dot{x}^2 + \dot{y}^2 + \dot{z}^2}{\dot{y}^2 + \dot{z}^2} \right]} + \frac{y_d^2}{R^2 \left[\frac{\dot{y}^2 + \dot{z}^2}{\dot{z}^2} \right]} = 1 \quad . \quad (D-11)$$

Since

$$P_{lap} = \frac{d}{\Delta S} \quad ,$$

then

$$d^2 = P_{lap}^2 \Delta S^2 \quad . \quad (D-12)$$

Substituting (D-12) into (D-11) yields

$$\frac{P_{lap}^2}{4R^2 \left[\frac{\dot{x}^2 + \dot{y}^2 + \dot{z}^2}{\dot{y}^2 + \dot{z}^2} \right] \Delta S^2} + \frac{y_d^2}{R^2 \left[\frac{\dot{y}^2 + \dot{z}^2}{\dot{z}^2} \right]} = 1 \quad . \quad (D-13)$$

The altitude difference, y_d , can be expressed as a linear function of η (the true anomaly at which the intersection line occurs) by writing the expression for y_d as a Taylor series. The expression for y_d is

$$y_d = f(\eta) = \frac{P}{1 + e \cos \eta} - R_t \quad . \quad (D-14)$$

The Taylor series of $f(\eta)$ expanded about the point η_o is

$$f(\eta) = f(\eta_o) + f'(\eta_o) (\eta - \eta_o) + \frac{f''(\eta_o)}{2!} (\eta - \eta_o)^2 + \dots \quad . \quad (D-15)$$

Substituting (D-14) into (D-15) and neglecting higher order terms (for small $\Delta\eta$'s) yields

$$y_d = \left[\frac{P}{1 + e \cos \eta_o} - R_t \right] - \left[\frac{P(1 - e \sin \eta_o)}{(1 + e \cos \eta_o)^2} \right] \Delta\eta \quad , \quad (D-16)$$

where

$$\Delta\eta = \eta - \eta_o \quad .$$

This linear function is a close approximation to the actual function if $\Delta\eta$ is sufficiently small. A typical value for $\Delta\eta$ is less than .5 deg.

Letting the constants in equation (D-16) be

$$a = \frac{P}{1 + e \cos \eta_o} - R_t \quad (D-17)$$

and

$$b = \frac{-P(1 - e \sin \eta_o)}{(1 + e \cos \eta_o)^2} \quad , \quad (D-18)$$

equation (D-16) then becomes

$$y_d = a + b \Delta\eta \quad . \quad (D-19)$$

If η_o is chosen such that $a = 0$ [equation (D-17)], then

$$y_d = b \Delta\eta \quad . \quad (D-20)$$

Substituting equation (D-20) into equation (D-13) yields

$$\frac{P_{lap}^2}{\frac{4R^2}{\Delta S^2} \left[\frac{\dot{x}^2 + \dot{y}^2 + \dot{z}^2}{\dot{y}^2 + \dot{z}^2} \right]} + \frac{R^2}{b^2} \left[\frac{\Delta\eta^2}{\dot{z}^2} \right] = 1 \quad . \quad (D-21)$$

This equation shows that the probability of collision versus η curve is elliptically shaped under the assumptions that (a) the velocity components of the debris satellite remain constant over the width ($\Delta\eta$) of the ellipse, and (b) the interval $\Delta\eta$, for which a non-zero probability exists, is sufficiently small to insure that y_d is a linear function of η . These assumptions are not true only

when the debris satellite radius of perigee is within several target sphere radii, R , of the radius of the target satellites orbital radius.

APPENDIX E

EXTENSION OF PROBABILITY PER LAP EXPRESSION TO PROBABILITY FOR THE ENTIRE MISSION

Let \bar{P}_{lap} be the probability, for each lap, that a debris satellite will collide with the target satellite. The probability, then, that a collision will not occur during the first lap of the mission is $1 - \bar{P}_{\text{lap}}$. The theorem of compound probability states that if A and B are any two independent events, then

$$p(AB) = p(A) p(B) \quad . \quad (E-1)$$

Stating equation (E-1) informally, the probability that both A and B happen is the probability that A happens times the probability that B then happens. Now associating A with the probability of noncollision for the first lap and associating B with the probability of noncollision for the second lap, the probability of noncollision for both laps is

$$P_{\text{nc}} = (1 - \bar{P}_{\text{lap}_1}) (1 - \bar{P}_{\text{lap}_2})$$

or

$$P_{\text{nc}} = (1 - \bar{P}_{\text{lap}})^2 \quad , \quad (E-2)$$

since the probabilities of noncollision are equal for both laps ($\bar{P}_{\text{lap}_1} = \bar{P}_{\text{lap}_2}$). The probability of noncollision for L laps is then

$$P_{\text{nc}} = (1 - \bar{P}_{\text{lap}})^L \quad . \quad (E-3)$$

Since

$$P_{\text{collision}} + P_{\text{noncollision}} = 1 \quad , \quad (E-4)$$

then the probability of collision with the jth satellite for a mission duration consisting of L laps is

$$P_{m_j} = (1 - \bar{P}_{\text{lap}_j})^L \quad . \quad (E-5)$$

APPENDIX F

COLLISION PROBABILITY BETWEEN THE TARGET SATELLITE AND ANY ONE OF THE TOTAL NUMBER OF DEBRIS SATELLITES

Let P_{m_j} be the probability of collision between the target satellite and the j th debris satellite for the total mission. The objective is to derive an expression for the probability that a collision will occur with any debris object considering the entire debris population. The principle of compound probability as explained in Appendix E applies in this case also. The difference here is that the individual satellite probabilities, P_{m_j} , will not be equal in general.

Thus, the total collision probability is written as

$$P_{TOT} = 1 - \prod_{j=1}^{n_d} (1 - P_{m_j}) \quad .$$

where

n_d = the total number of debris satellites in earth orbit.

APPENDIX G

DETERMINATION OF THE ANGLE BETWEEN TWO ORBIT PLANES

Figure G-1 shows the projections of two orbit paths onto a spherical earth. The orbits represented by these projections are inclined to the equatorial plane by amounts i_d and i_t . The angle between the planes, δ , can be found in terms of the known quantities, i_d , i_t , and $\Delta\Omega$ by considering the oblique spherical triangle ABC. The relations between the sides and angles of this triangle are completely specified by Napier's analogies. The equations are as follows:

$$\frac{\sin \frac{1}{2} (i'_t - i_d)}{\sin \frac{1}{2} (i'_t + i_d)} = \frac{\tan \frac{1}{2} (\sigma - \lambda)}{\tan \frac{1}{2} (\Delta\Omega)} \quad (G-1)$$

$$\frac{\cos \frac{1}{2} (i'_t - i_d)}{\cos \frac{1}{2} (i'_t + i_d)} = \frac{\tan \frac{1}{2} (\sigma + \lambda)}{\tan \frac{1}{2} (\Delta\Omega)} \quad (G-2)$$

$$\frac{\sin \frac{1}{2} (\sigma - \lambda)}{\sin \frac{1}{2} (\sigma + \lambda)} = \frac{\tan \frac{1}{2} (i'_t - i_d)}{\cot \frac{1}{2} \delta} \quad (G-3)$$

$$\frac{\cos \frac{1}{2} (\sigma - \lambda)}{\cos \frac{1}{2} (\sigma + \lambda)} = \frac{\tan \frac{1}{2} (i'_t + i_d)}{\cos \frac{1}{2} \delta} \quad (G-4)$$

Equations (G-1), (G-2), and (G-4) are sufficient to find δ . First, solve equations (G-1) and (G-2) for $\frac{(\sigma - \lambda)}{2}$ and $\frac{(\sigma + \lambda)}{2}$ respectively, to obtain

$$\frac{(\sigma - \lambda)}{2} = \tan^{-1} \left[\sin \frac{1}{2} (i_t' - i_d) \csc \frac{1}{2} (i_t' + i_d) \tan \frac{1}{2} \Delta \Omega \right] \quad (G-5)$$

and

$$\frac{(\sigma + \lambda)}{2} = \tan^{-1} \left[\cos \frac{1}{2} (i_t' - i_d) \sec \frac{1}{2} (i_t' + i_d) \tan \frac{1}{2} \Delta \Omega \right] \quad (G-6)$$

Substituting equations (G-5) and (G-6) into (G-4) to eliminate the unknown quantities and then solving for δ yields

$$\delta = 2 \cot^{-1} \left[\tan \frac{1}{2} (i_t' + i_d) \cos \tan^{-1} (j) \sec \tan^{-1} (k) \right] \quad (G-7)$$

where

$$j = \cos \frac{1}{2} (i_t' - i_d) \sec \frac{1}{2} (i_t' + i_d) \tan \frac{1}{2} \Delta \Omega$$

and

$$k = \sin \frac{1}{2} (i_t' - i_d) \csc \frac{1}{2} (i_t' + i_d) \tan \frac{1}{2} \Delta \Omega \quad .$$

Noting from Figure G-1 that $i_t' = \pi - i_t$, and substituting this into equation (G-7) results in

$$\delta = 2 \cot^{-1} \left[\cot \frac{1}{2} (i_t - i_d) \cos \tan^{-1} (j') \sec \tan^{-1} (k') \right] \quad (G-8)$$

where

$$j' = \sin \frac{1}{2} (i_t + i_d) \csc \frac{1}{2} (i_t - i_d) \tan \frac{1}{2} \Delta \Omega$$

and

$$k' = \cos \frac{1}{2} (i_t + i_d) \sec \frac{1}{2} (i_t - i_d) \tan \frac{1}{2} \Delta \Omega \quad .$$

APPROVAL

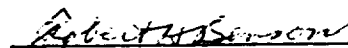
PROBABILITY OF SATELLITE COLLISION


By James W. McCarter

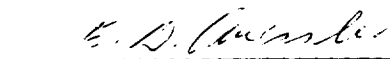
The information in this report has been reviewed for security classification. Review of any information concerning Department of Defense or Atomic Energy Commission programs has been made by the MSFC Security Classification Officer. This report, in its entirety, has been determined to be unclassified.

This document has also been reviewed and approved for technical accuracy.


BARTON S. PERRINE, JR.
Chief, Mission Design Section


ROBERT H. BENSON
Chief, Orbital Mechanics Branch


JAMES P. LINDBERG
Chief, Mission Planning and Analysis Division


E. D. GEISSLER
Director, Aero-Astroynamics Laboratory

REFERENCE

1. Satellite Situation Report. Office of Public Affairs, GSFC, vol. XI, no. 10, Oct. 31, 1971.

INTERNAL

DIR S&E-AERO-M
Mr. Lindberg (2)

DEP-T S&E-AERO-MM
Mr. Benson (2)
Mr. Haussler

As TS-PA1
Mr. Wolford

PM-PR-M S&E-AERO-NMD
Mr. Perrine (20)
Mr. McCarter (25)

Mr. Goldston S&E-AERO-MX
Mr. Crenan

AS TS-MS-H S&E-AERO-MF
Mr. Hardage

AS TS-MS-IP (2) S&E-ASTN-X
Mr. Platt

AS TS-MS-IL (8) S&E-AERO-R
Mrs. Hightower

AS TS-TU S&E-ASTN-S
Mr. Isbell

Mr. Wygans (6) S&E-CSE-DIR
Mrs. Hightower

AD-S S&E-ASTN-PPC
Mr. Jones

Dr. Stuhlinger (6) S&E-CSE-A
Mr. Higgins
Dr. Geissler
Mr. Horn

S&E-AERO-DIR S&E-CSE-V
Mr. Tinius

S&E-AERO-T S&E-CSE-G
Mr. Currie

Mr. Murphree S&E-AERO-P
Mr. Beam
Mr. Verderaine

Mr. Sims S&E-CSE-V
Mr. Smith

Mr. Jackson S&E-ASTR-B
Mr. Kampmeier

Mr. Gibbons S&E-ASTR-S
Mr. Brooks

S&E-AERO-A S&E-ASTR-SI
Mr. Tanner

Mr. Dahm S&E-ASTR-SDA
Mr. Justice

S&E-AERO-D S&E-ASTR-SL
Mr. Cox

Dr. Lovingsood S&E-AERO-DO
Mr. Brooks

Dr. Worley S&E-ASTR-SI
Mr. Rankin

S&E-AERO-Y S&E-ASTR-SDA
Mr. Justice

Mr. Vaughn S&E-ASTR-SL
Mr. Cox

S&E-AERO-Y S&E-ASTR-SL
Mr. Cox

S&E-AERO-G S&E-ASTR-SL
Mr. Cox

Mr. Baker S&E-ASTR-SL
Mr. Cox

Mr. Elrod S&E-ASTR-SL
Mr. Cox

PM-HE-MGR
Dr. Speer

PD-SS-MGR
Mr. Brooksbank
Mr. Palastro
Mr. Lavender
Mr. Dannenberg
Mr. Bramlet

PD-SS-1
Mr. Keller
Mr. Brown

PD-PS-DIR
Mr. Lucero

PD-SA-DIR
Mr. Huber

PD-MP-DIR
Mr. Gierow

PD-DO-DIR
Mr. Goerner

PD-RV-MGR
Mr. Dean

PD-MP-A
Mr. Neun

PD-ID-DIR
Mr. Smith

PD-ID-1
Mr. Smith

PD-DO-1
Mr. Goldsby

EXTERNAL

National Aeronautics and Space Agency
NASA Headquarters
Washington, D. C. 20546

Attn: Dr. von Braun

Mr. Gillooly, MLO

Mr. Armstrong, MTX

Mr. E. Hall, MTG

Mr. W. Hall, MT-1

Mr. H. Hall, MT-2

Mr. Huff, MTE

Mr. Keegan, MTE

Mr. Wild, MTE

Mr. Schuyler, MTE

Mr. Johnson, MF

Mr. Lohman, MF

Mr. Lord, MF

Dr. Johnson, MF

Mr. Lindsey, M

Mr. Lyman, MR

Mr. Moore, MH

Mr. Summerfelt, MH

Mr. Shaw, DY

Mr. Alder, MAO

Mr. McCannan, MAO

Mr. Evans, WLO

Mr. Beverly, TN

Mr. Day, MB

NASA
Manned Spacecraft Center
Houston, Tex. 77001

Attn: Mr. Allen, FM3

Mr. Donahoe, FM3

Mr. Everline, HB

Mr. Hicks, FA4

Mr. Huss, FM

Mr. McPherson, FM4

Mr. Berry, FM5

Mr. Hunt, FM3

Mr. Litterton, KM

Mr. Young, FM6

Mr. Williamson, FM3

Mr. Thompson, KA

IBM Corporation
150 Sparkman Dr., N. W.
Huntsville, Ala. 35895

Attn: Mr. Robinson

Mr. Hyle

Mr. Chatterpa

Mr. Nelson

Mr. McDonald

Mr. Hyle

Mr. Ryan

General Dynamics/Convair
P. O. Box 1128
San Diego, Calif. 92112

Attn: Mr. Macdonald

Mr. Chatterpa

Mr. Nelson

Mr. McDonald

Mr. Hyle

Mr. Ryan

Northrop Corp.
6025 Technology Dr.
Huntsville, Ala. 35895

Attn: Mr. Klumbur

Mr. Haney

Mr. Hurst

Mr. Spencer

North American Rockwell Corporation
12214 Lakewood Boulevard
Downey, Calif. 90241

Attn: Mr. Logsdon

Mr. Garch

Mr. Burnett

TRW Systems
One Space Park
Redondo Beach, Calif. 90276

Attn: Mr. Brown

Mr. Burnett

Mr. Waltz

Scientific & Technical Information
Facility (23)
P. O. Box 33
College Park, Md. 20740

Attn: NASA Representative (S-AK HKT)

DISTRIBUTION

W. G. Hedron

Mr. Rice, WD

Mr. Davis, WD

Mr. Biel, WD

Mr. Gathel, WD

Mr. Alderson, WD

Mr. Bess

Mr. Matersick

Mr. Bess

Mr. Matersick

Mr. Bess

Mr. Matersick

Mr. Bess

Mr. Matersick

Mr. Bess

Mr. Matersick

Mr. Bess

Mr. Matersick

Mr. Bess

Mr. Matersick

Mr. Bess

Mr. Matersick

Mr. Bess

Mr. Matersick

Mr. Bess

Mr. Matersick

Mr. Bess

Mr. Matersick

Mr. Bess

Mr. Matersick

Mr. Bess

Mr. Matersick

Mr. Bess

Mr. Matersick

Mr. Bess

Mr. Matersick

Mr. Bess

Mr. Matersick

Mr. Bess

Mr. Matersick

Mr. Bess

Mr. Matersick

Mr. Bess

Mr. Matersick

Mr. Bess

Mr. Matersick

Mr. Bess

Mr. Matersick

Mr. Bess

Mr. Matersick

Mr. Bess

Mr. Matersick

Mr. Bess

Mr. Matersick

Mr. Bess

Mr. Matersick

Mr. Bess

Mr. Matersick

Mr. Bess

Mr. Matersick

Mr. Bess

Mr. Matersick

Mr. Bess

Mr. Matersick

Mr. Bess

Mr. Matersick

Mr. Bess

Mr. Matersick

Mr. Bess

Mr. Matersick

Mr. Bess

Mr. Matersick

Mr. Bess

Mr. Matersick

Mr. Bess

Mr. Matersick

Mr. Bess

Mr. Matersick

Mr. Bess

Mr. Matersick

Mr. Bess

Mr. Matersick

Mr. Bess

Mr. Matersick

Mr. Bess

Mr. Matersick

Mr. Bess

Mr. Matersick

Mr. Bess

Mr. Matersick

Mr. Bess

Mr. Matersick

Mr. Bess

Mr. Matersick

Mr. Bess

Mr. Matersick

Mr. Bess

Mr. Matersick

Mr. Bess

Mr. Matersick

Mr. Bess

Mr. Matersick

Mr. Bess

Mr. Matersick

Mr. Bess

Mr. Matersick

Mr. Bess

Mr. Matersick

Mr. Bess

Mr. Matersick

Mr. Bess

Mr. Matersick

Mr. Bess

Mr. Matersick

Mr. Bess

Mr. Matersick

Mr. Bess

Mr. Matersick

Mr. Bess

Mr. Matersick

Mr. Bess

Mr. Matersick

Mr. Bess

Mr. Matersick

Mr. Bess

Mr. Matersick

Mr. Bess

Mr. Matersick

Mr. Bess

Mr. Matersick

Mr. Bess

Mr. Matersick

Mr. Bess